ASSESSING FUNCTIONAL STABILITY OF PREDICTED MUSCLE ACTIVATION PATTERNS FOR POSTURAL CONTROL USING A NEUROMECHANICAL MODEL OF THE CAT HINDLIMB

A Thesis
Presented to
The Academic Faculty

by

Mark Hongchul Sohn

In Partial Fulfillment
of the Requirements for the Degree
Master of Science in the
Woodruff School of Mechanical Engineering

Georgia Institute of Technology
December 2011

ASSESSING FUNCTIONAL STABILITY OF PREDICTED MUSCLE ACTIVATION PATTERNS FOR POSTURAL CONTROL USING A NEUROMECHANICAL MODEL OF THE CAT HINDLIMB

Approved by:

Dr. Lena Ting, Advisor
Coulter Department of Biomedical Engineering
Emory University and Georgia Institute of Technology

Dr. Jun Ueda
Woodruff School of Mechanical Engineering
Georgia Institute of Technology

Dr. Thomas Burkholder
School of Applied Physiology
Georgia Institute of Technology

Dr. Aldo Ferri
Woodruff School of Mechanical Engineering
Georgia Institute of Technology

Date Approved: August 18, 2011

Soli Deo Gloria

ACKNOWLEDGEMENTS

I would like to first thank my advisor, Dr. Lena Ting for giving me such a great opportunity to work with her on this exciting project. Along the way, she has been a boss with patience, a generous mentor, an inspiring teacher, and a sincere friend to me. Most of all, she has taught me not only how to solve a problem but also how to cast one. I am also grateful to my committee, Dr. Thomas Burkholder, Dr. Also Ferri, and Dr. Jun Ueda. Their comments and suggestions provided a broader aspect on the problem.

I can never thank my lab enough for their supports. I thank Dr. J. Lucas McKay for his guidance, devoting his time and effort to help me break through the walls. I thank Jeff Bingham for always being there for an insightful advice, whether scientific or technical. I thank Seyed Safavynia and Dr. Stacie Chvatal for their feedbacks that kept me on the track. I thank Dr. Julia Choi, Keith van Antwerp and D. Joseph Jilk for being such a helpful reviewer. Few, outside the lab, I would like to express my appreciation for are the modelers. I thank Dr. T. Richard Nichols, Dr. Nate Bunderson, and Ramaldo Martin for their interest in the project and providing valuable comments on every detail.

To my family, whom I have debt of prayers throughout the life, I want to prove to them the reason for being back here at Atlanta. The members of New Church of Atlanta, so many to mention, has given me strength and comfort.

Lastly, I want to thank Jinhee Kim for being there beside me in any circumstances. Ever since she has walked into my life, I am willing to change to be a better person, which is a miracle for such an unteachable man like me.

Thank you all.

Studying neural control of movement has always amazed me as I witness the beauty of the design which is all so wondrous. Even though all I could seek for my entire life would still be only a tiny bit of the whole, I shall walk this path humbly in recognition of the Designer who resides above. All is Yours, and You are my all.

TABLE OF CONTENTS

LIST OF TABLES

LIST OF FIGURES

SUMMARY

The underlying principles of how the nervous system selects specific muscle activation pattern, among many that produce the same movement, remain unknown. Experimental studies suggest that the nervous system may use fixed groups of muscles, referred to as muscle synergies, to produce functional motor outputs relevant to the task. In contrast, predictions from biomechanical models suggest that minimizing muscular effort may be the criteria how a muscle coordination pattern is organized for muscle synergies. However, both experimental and modeling evidence shows that stability, as well as energetic efficiency, also needs to be considered.

Based on the hypothesis that the nervous system uses functionally stable muscle activation pattern for a muscle synergy, we investigated the stability of muscle patterns using a neuromechanical model of the cat hindlimb. Five unique muscle patterns that generate each of the five experimentally-identified muscle synergy force vectors at the endpoint were found using a minimum-effort criterion. We subjected the model to various perturbed conditions and evaluated functional stability of each of the five minimum-effort muscle synergies using a set of empirical criteria derived from experimental observations.

Results show that minimum-effort muscle synergies can be functionally stable or unstable, suggesting that minimum-effort criterion is not always sufficient to predict physiologically relevant postural muscle synergies. Also, linearized system characteristics can robustly predict the behavior exhibited by fully dynamic and nonlinear biomechanical simulations. We conclude that functional stability, which assesses stability

of a biomechanical system in a physiological context, must be considered when choosing a muscle activation pattern for a given motor task.

CHAPTER 1

INTRODUCTION

1.1 Muscle coordination

The control of movement in humans or in animals is a complex task which requires coordination of muscles that span multiple anatomical degrees of freedom (DoF). At the execution level, the nervous system controls movement by exciting particular muscles to contract through neural signals in the form of an action potential. A movement is induced by the pulling actions of multiple muscles which in turn produce the net torque at the rotational joints. Subsequently, torque at each of the multiple joints contributes to either acceleration of the body segments and/or production of a force against the environment in a given configuration. Thus the smooth and dexterous movement in human requires the coordination of multiple muscles across the body working in harmony both in spatial and temporal aspects.

However, due to musculoskeletal redundancy in that the number of muscles exceeds the number of degrees of freedom (DoF) to be controlled, any movement can be produced with multiple muscle coordination patterns (Berstein, 1967). Therefore, muscle patterns to produce a given movement must be selected from an infinite number of possible solutions. However, the nervous system seems to use not just any solution randomly chosen from the pool for a given motor task, but rather coordinates the muscles in a specific manner which results in functional behavior that is consistent and robust. In standing balance of humans and animals, stereotypical muscle activation patterns are observed for multi-directional perturbations (Henry et al., 1998; Macpherson 1998). In human walking, consistent pattern of muscle activity is observed during specific phase of the gait cycle (Carlsoo, 1972; Mann et al., 1979; Winter, 1987; Winter and Yak, 1987;

Elble et al., 1994). A major question that had remained unanswered for decades in the study of neural control of movement is the underlying principle of how the nervous system coordinates the muscles in a specific way, resolving the redundancy problem.

1.2 Muscle synergy hypothesis

Studies suggest that the nervous system may use a few sets of solutions, reducing the number of independent degrees of freedom that must be controlled. This hypothesis has been mainly supported by identification of a small number of groups of muscles with fixed ratios of activation called muscle synergies which can account for the large number of electromyographic (EMG) activities examined during motor behaviors. Muscle synergies have been found in various motor tasks such as locomotion (Ivanenko et al., 2003; Drew et al., 2008) and reaching (d'Avella et al., 2006), natural behaviors of frogs (Tresch et al., 1999; d'Avella et al., 2003; Hart and Giszter, 2004), and standing balance in cats and humans (Ting and Macpherson, 2005; Torres-Oviedo and Ting, 2007). Various computational analyses, which are mainly matrix factorization algorithms, are used to extract muscle synergies (review in Tresch et al., 2006).

Recent studies from our laboratory identified postural muscle synergies and related synergy force vectors that were sufficient to explain the activation of muscles and limb forces during unrestrained balance control tasks in both cats (Torres-Oviedo et al., 2006) and humans (Chvatal et al., 2011). Results from these studies suggest that the organization of muscle synergies is robust across different biomechanical contexts. Other studies have also shown that common muscle synergies are used in various motor tasks with different dynamics (Ivanenko et al., 2005, d'Avella and Bizzi, 2005; Torres-Oviedo and Ting, 2010). However, how the nervous system selects specific muscle pattern for muscle synergies remain unknown.

1.3 Minimum–effort solutions

One popular hypothesis of how the nervous system selects muscle activation patterns is that it may minimize the amount of muscular effort. This suggests that muscle synergy may also be structured for energetic efficiency as well. Because many patterns of muscle activity can produce equivalent patterns of joint torque or limb endpoint force, many studies identify unique muscle patterns by the minimization of cost functions based on some physiological criteria. In particular, minimizing the sum amount of muscle activation has been most widely accepted since the work of Crowninshield and Brand in 1971. This optimality principle has been applied in various forms for various motor tasks specifically in studies using biomechanical modeling and simulations to predict muscle coordination of movement (review in Erdemir et al., 2007; Thelen et al., 2003; Thelen and Anderson, 2006).

However, observations particularly in dynamic aspects of movement reveal that minimization of muscle activation may produce functional outputs that are unstable, suggesting that stability may also be important in selecting muscle synergy structure. Experimental studies suggest that subjects may trade off effort expenditure for stability during motor tasks (Franklin et al., 2008; Hunter et al, 2010; Ganesh et al., 2010), suggesting that these two objectives may conflict. This idea is also supported by modeling results that demonstrate that minimizing muscle activation predicts motor patterns that are in qualitative agreement with experimental measurements. However, sensitivity analyses on the predicted solutions have also showed that the results may depend critically on factors such as modeling parameters, description of joint kinematics or accuracy of the data used (Vaughan et al., 1982; Kuo, 1998; Li et al., 1999). Further, solutions from static predictions can make the system unstable when applied to the dynamic model. Dynamic predictions that track prescribed motion as well as minimize energetic expenditure can also become unstable with more challenging conditions such as introducing perturbations or applying the model in three dimensions (Jinha et al., 2006).

It has been shown that different muscle activation patters that satisfy static generation of stance-like force in a three-dimensional dynamic model of the cat hindlimb differ in intrinsic stability conferred to the limb, defined by the sign of the eigenvalue in system linearized at an initial equilibrium (Bunderson et al., 2008). It was further shown that a minimum effort solution yields instability in generation of the output force when subjected to dynamic perturbation (Bunderson et al., 2010). Therefore, for a predicted muscle pattern for muscle synergy to be a viable solution, it is likely that it must exhibit functional stability where it incorporates the robustness in production of its functional motor output.

1.4 Defining functional stability

Functional stability can be described as the production of consistent behavioral output within the physiological context of movement control. For example, in balance control, being functionally stable can be considered as generating an appropriate force against the ground in a robust manner, without substantial changes in the limb configuration. However, assessing or even defining stability of a complex and highly nonlinear biomechanical system is not trivial. Although conventional tools of linear systems control provide approximate predictions of the local dynamic behavior of such systems, it may not always be physiologically relevant. Stability in a most strict sense will often determine a biological system to be unstable because the system's response, observed in both musculature and neural circuitry, do not always oppose the perturbation (Hasan, 2005). Limitations also lie in the extent to which linearization is effective regarding the contributions from various neuromechanical constituents of movement stability such as biomechanical constraints of anatomical joints, intrinsic muscle properties, multi-layered feedback loops with different latencies, and sensori-motor integration.

More importantly, the nervous system cannot react instantly because there exist delays in conduction of the sensorimotor signals which can be a destabilizing factor in terms of feedback control. However, during perturbations to standing balance, the background muscle activity itself limits the small joint angle changes in the first 100 ms following a perturbation (Jacobs and Macpherson, 1996), which represents the neurological timescale where sensorimotor corrections are absent. Therefore, the metrics of functional stability in balance control should define the range of the behavioral motor outputs that can be corrected in neurological timescales to produce physiologically consistent behaviors, rather than providing an absolute stability over irrelevant timescale.

1.5 Rationale and overview of the study

It has not been demonstrated whether any behavior under muscle synergy control can still be stable in dynamic aspects, especially in the presence of perturbation to the system. In postural responses to standing balance in cats, five muscle synergies were identified to produce consistent force outputs across animals (Torres-Oviedo et al., 2006). The plausibility of such solutions robustly producing the same force across different biomechanical contexts was further demonstrated using a detailed three-dimensional static model of the hindlimb (McKay and Ting, 2008). However, muscle synergy structure for a given force vector showed variability across animals in the experiments. Also, using different criteria for selecting the muscle pattern for a given force vector resulted in drastically different solutions in the static model. Redundancy as demonstrated in the biomechanical solution space leaves possibility of a neural constraint regarding functional stability to be imposed, because stability of the limb is affected by the intrinsic stiffness properties of active muscles (Bunderson et al., 2008).

Based on the hypothesis that the nervous system uses functionally stable muscle activation pattern for a muscle synergy, we investigated system stability of given muscle

patterns using a neuromechanical model of the cat hindlimb. In order to first test the feasibility whether a solution can be functionally stable, five unique muscle patterns that generate each of the five experimental muscle synergy force vectors at the endpoint were found using the sum of muscular effort, activation squared, as the minimizing criteria. We subjected the model to various perturbed conditions and evaluated stability of each of the five minimum-effort muscle synergies using a set of empirical criteria derived from experimental observations. Specifically, we present a set of criteria for functional stability defined to maintain the deviations in the joint kinematic states and the output force vector within certain ranges for a certain period of time when the system is perturbed near the equilibrium of static force generation (see METHODS for details). Finally, in an attempt to relate the well-known methods of estimating the local dynamic stability to the actual behavior of the biomechanical system, we test whether linearized system characteristics can predict functional stability in a physiological sense.

CHAPTER 2

METHODS

2.1 Overview

A detailed neuromechanical model of the cat hindlimb with posture matched to the kinematics of a cat standing in its preferred stance was used to simulate the dynamic behavior of the system driven by muscle patterns that were tested for functional stability. Five muscle synergy patterns that produced each of the five corresponding synergy force vectors found from a previous experimental study were identified with static optimization using minimum energetic expenditure as the cost function. These minimum effort muscle synergy patterns were then used as a constant input to the muscles in the model. Forward dynamic simulations were run with joint configurations which varied around the original posture. The resulting behavior of the system in response to each perturbation was subjected to the criteria we present for assessing the relationship between muscle activation patterns and functional stability for postural control of a cat. We then tested whether the eigenvalues and eigenvectors of the system linearzed about an equilibrium point at the original posture could predict each the Lyapunov stability and the functional stability of the perturbed system.

2.2 Hindlimb muculoskeletal model

In order to assess the functional stability of a muscle activation pattern, we used a realistic model of the cat hindlimb (Fig. 1). The three-dimensional model of the right hindlimb was originally built based on the anatomical measurements of muscle attachments and mechanical identification of joint locations (Burkholder and Nichols,

2000 and 2004). Briefly, the model used in this study has seven rotational degrees of freedom at the anatomical joints: hip flexion (HF), hip adduction (HA), hip rotation (HR), knee extension (KE), knee adduction (KA), ankle extension (AE) and ankle adduction (AA). The axes of rotation are orthogonal to each other only at the hip where axes at the knee and ankle are non-orthogonal non-intersecting. The pelvis is fixed to the ground for all six degrees of freedom and the limb endpoint contacting the ground, defined as the metatarsophalangeal (MTP) joint location, is modeled as a pin joint constraining the three degrees of freedom in translation (Fig. 1B). The default joint configuration was adjusted to match the normal preferred stance-like posture of the cat *Russl* measured from a previous postural balance experiment (Jacobs and Macpherson 1996, Ting and Macpherson, 2005; McKay et al., 2007). The coordinate frame was defined as X axis being anterior-posterior (AP) direction, Y axis the vertical direction and Z axis the medial-lateral (ML) direction (Fig. 1A).

The equation of motion, in a matrix-vector form, that describes the dynamic behavior of the hindlimb system in generalized coordinate system of the joint angles $\vec{q} = [q_{\mathrm{HF}}, q_{\mathrm{HA}}, q_{\mathrm{HR}}, q_{\mathrm{KE}}, q_{\mathrm{KA}}, q_{\mathrm{AE}}, q_{\mathrm{AA}}]^T$ can be given as,

$$\mathbf{M}(\vec{q})\ddot{\vec{q}} = \mathbf{R}(q)\vec{F}_M(\vec{q}, \dot{\vec{q}}, \vec{a}) - \mathbf{J}(\vec{q})^{\mathbf{T}}\vec{F}_{End} - \vec{V}(\vec{q}, \dot{\vec{q}}) - \vec{G}(\vec{q}) \qquad (1)$$

where $\dot{\vec{q}}$ and $\ddot{\vec{q}}$ are the joint velocity and acceleration vector respectively; $\vec{a}$ is the muscle activation pattern; **M** is the inertia matrix; **R** is the moment arm matrix; **J** is the endpoint Jacobian; $\vec{F}_M$ is the vector of muscle forces; $\vec{F}_{End}$ is the vector of endpoint forces; $\vec{V}$ is the vector of Coriolis terms; and $\vec{G}$ is the gravitational torque vector. However, in order to examine independently the production of the endpoint forces generated by specific muscle activation patterns, the gravitational term was ignored.

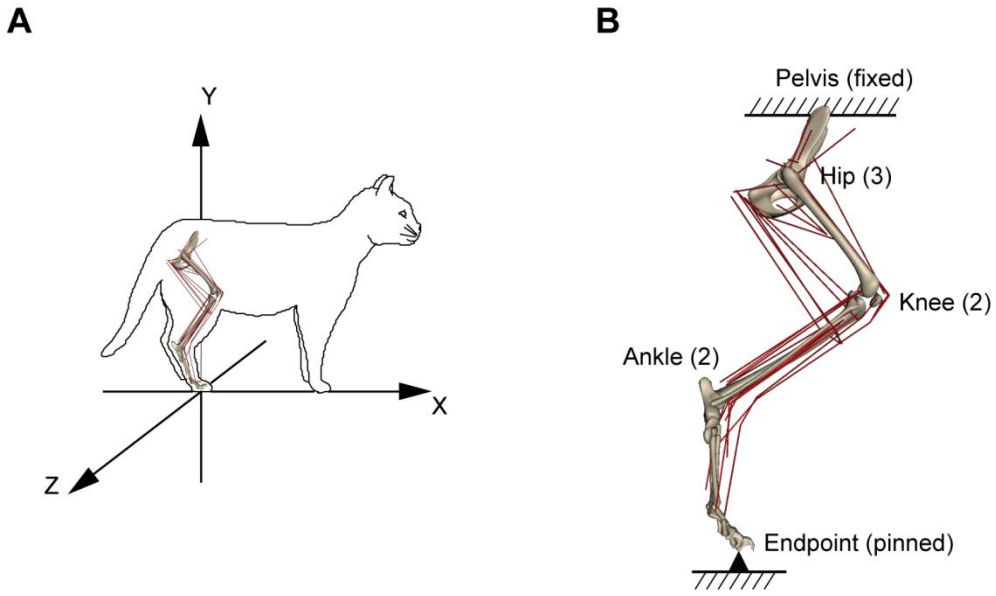

Figure 1. Schematic of the hindlimb musculoskeletal model. **A:** Coordinate frame is defined as positive X, Y, and Z directions being in the anterior, vertical up, and medial direction respectively. **B:** The model has seven degrees of freedom at the anatomical joints: three at the hip, two at each knee and ankle. The pelvis is fixed to the ground where the limb endpoint is modeled as pin joint.

For the 31 muscles in the hindlimb model (list and abbreviations in Table 1), Hill-type muscle model with inelastic tendons and angle of pennation (Zajac, 1989) was used (Fig. 2A). In particular, muscle force is composed of active and passive components, both based on the current state of the musculo-tendon length (MTL) and velocity (MTV) each normalized to the optimal fiber length (L_F/L^0_F) and maximum fiber shortening velocity (V_F/V^{max}_F) respectively. Generated active muscle force is proportional to point on the nonlinear curve for MTL and MTV, which is then linearly scaled by the level of muscle activation and maximum isometric contractile force specified for each muscle (Eq. 2). Since muscle fiber length and velocity are determined by the posture, intrinsic stiffness in terms of resisting force with respect to change in posture is introduced by the characteristic force versus fiber length and velocity curve (Fig. 2B). At given configuration, stiffness property of both the joint and the whole limb is determined by the muscle activation because muscle activation linearly scales the force producing characteristics of the muscle. In this study, each muscle was set to have fiber lengths at 65% of its optimum in the default posture by specifying a specific value for the tendon slack length. With the value 65%, intrinsic stiffness is defined to be about $3F_{max}/L^0_F$ which is near the maximal stiffness that can be found from the force-tension relationship curve (Gordon et al., 1966).

$$F_M = F_{Max}[afl(L_F/L^0_F)\cdot afv(V_F/V^{max}_F)\cdot a + pfl(L_F/L^0_F) + \eta(V_F/V^{max}_F)]\cos\alpha_{penn} \quad (2)$$

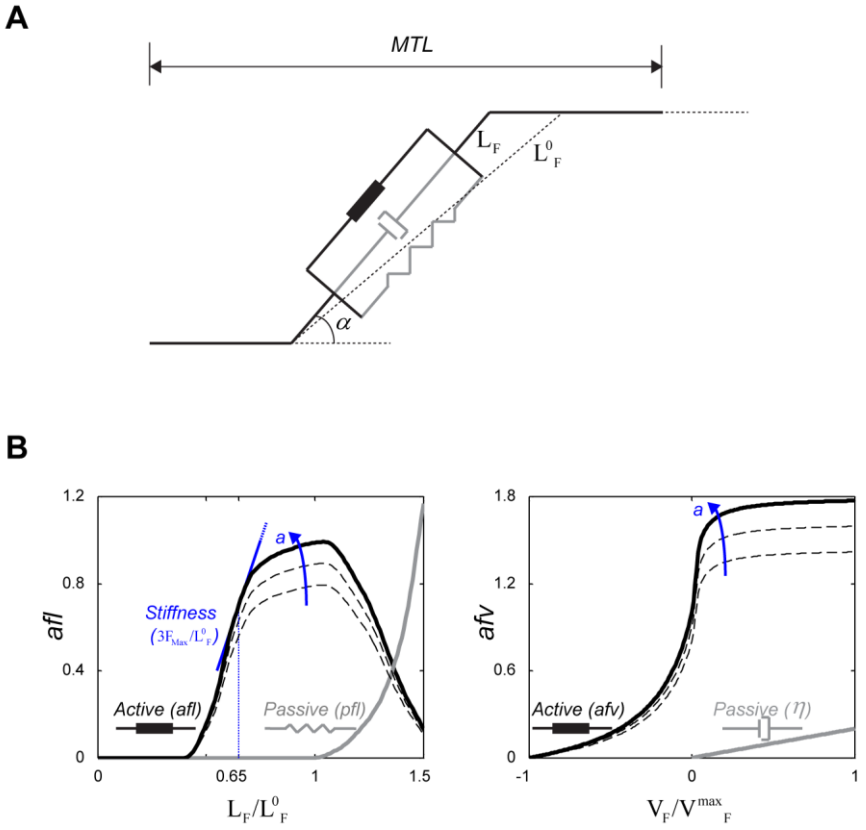

Figure 2. Schematic of the muscle model and active muscle force generation. **A:** The model takes into account of pennation angle of each muscle and has passive and active contractile component. **B:** Muscle force generation as a function of fiber length, fiber velocity and muscle activation. Muscle activation scales (blue arrow) the active force generated given a state of fiber length and velocity. Force-length relationship provides intrinsic stiffness to the change in musculo-tendon length (MTL) which can be represented with the slope at any point on the curve. Fiber lengths were set to be at 65% of its optimum for all muscles providing stiffness about $3F_{max}/L^0_F$ at the default posture (blue line).

Table 1. Muscles included in the hindlimb model and abbreviations.

Name	Abbreviation	Name	Abbreviation
Adductor femoris	ADF	*Plantaris*	PLAN
Adductor lounges	ADL	*Psoas minor*	PSOAS
Biceps femoris anterior	BFA	*Peroneus tertius*	PT
Biceps femoris posterior	BFP	*Pyriformis*	PYR
Extensor digitorum longus	EDL	*Quadratus femoris*	QF
Flexor digitorum longus	FDL	*Rectus femoris*	RF
Flexor hallucis longus	FHL	*Sartorius*	SART
Gluteus maximus	GMAX	*Semimembranosus*	SM
Gluteus medius	GMED	*Soleus*	SOL
Gluteus minimus	GMIN	*Semitendinosus*	ST
Gracilis	GRAC	*Tibialis anterior*	TA
Lateral gastrocnemius	LG	*Tibialis posterior*	TP
Medial gastrocnemius	MG	*Vastus intermedius*	VI
Peroneus brevis	PB	*Vastus lateralis*	VL
Pectineus	PEC	*Vastus medius*	VM
Peroneus longus	PL		

2.3 Muscle activation pattern selection

Five unique muscle activation patterns that generate each of the five experimental synergy force vectors were found using a quadratic cost function that summed squared activation of the muscles (Eq. 3.1). The synergy force vectors (SFVs) used in this study were from left hindlimb of the cat *Russl* (Fig. 4A) and were transformed symmetric to the sagittal plane to be applied to the right hindlimb model. Magnitude of the five SFVs magnitude varied from 0.12 N to 3.09 N where maximum feasible force (McKay et al., 2007; McKay and Ting, 2008) in any of the directions for SFVs was considerably larger qualitatively. Since all SFVs were within the manifold of biomechanical capability of the endpoint force production in the hindlimb model, unique minimum-effort solution was guaranteed feasible for all muscle synergies.

An equality constraint was formed from the equations of motion so that joint torque generated by the muscle activation satisfies the joint torque that is specified by each SFV (Eq. 3.2). Motion-dependent effects were excluded from the constraint equation because experimental synergy force vectors are static forces extracted by averaging across specific time window of the automatic postural response: 80 ms window following 120 ms after the onset of the perturbation. In addition, muscle activation is modeled to be any number between 0 and 1 which represents the physiological bound for muscle activation. In practice, 10E-5 and 0.95 were used as the lower and upper bound for the solution respectively (Eq. 3.3). It was found that having smaller lower bound did not further alter the solution (result not reported here). In summary, static optimization problem is formulated as below;

- Cost function: $$\min \sum_{m=1}^{31} {a_m}^2 \quad (3.1)$$
- Equality constraint: $$\mathbf{RF_M}\,\overrightarrow{a_i} = \mathbf{J^T}\,\overrightarrow{SFV}_i \quad (3.2)$$
- Inequality constraint: $$10^{-5} \le a_i \le 0.95 \quad (3.3)$$

$\mathbf{R}$ is a 7x31 moment arm matrix that maps muscle force to net torque generated at the joints. $\mathbf{F_M}$ is a diagonal matrix with the active force generating characteristics of each muscle. Results from above optimization were used as constant neural input to the system: muscle activations.

2.4 Dynamic response to perturbations

In order to investigate the stability of the identified muscle activation patterns, the system was perturbed by varying the initial configuration of the model in two different methods (Fig. 4). The first perturbation type (Type I) was designed to resemble changes in the relative horizontal distance between the pelvis and endpoint observed in the experiments. Center of mass (CoM) displacement relative to the feet was typically about 2 cm after 200 ms following the onset of the perturbation (Ting and Macpherson 2004). CoM displacement relative to the position of the feet in a freely standing cat is equivalent to the feet displacement relative to the fixed pelvis in the model. Therefore, the endpoint position was displaced between -20 mm to 20 mm in 1 mm increment along the four uniformly distributed axes in the horizontal plane: XX (positive in anterior and negative in posterior direction), ZZ (positive in lateral and negative in medial direction), XZ (diagonal, 45° to positive XX direction) and ZX (diagonal, orthogonal to XZ). The metric $\|\Delta q\|$, which is the root-mean-square (RMS) of the deviations at the seven joint angles, was used to measure the overall deviation in the joint configuration. In Type I perturbation, it was shown that $\|\Delta q\|$ was less than 5° for all conditions.

The second type of perturbation (Type II) was designed to replicate changes in individual joint angles given a fixed distance between the pelvis and the endpoint. The variability in individual joint angle during the cat experiment was shown to be typically about ±5° (Fung and Macpherson, 1995). Therefore, in Type II perturbation, each of the

seven joint angles (HF, HA, HR, KE, KA, AE and AA) was modulated to 10 uniform intervals each in negative and positive direction while maintaining the endpoint position the same as the default posture. However, applying a common interval for all of the joints do not perturb the overall configuration in a consistent range because joints are inter-coupled together either mechanically or by muscle activation within given muscle coordination. For example, changes at the proximal joints such as hip flexion may further affect the distal joints such as ankle extension at a larger extent. Therefore, interval size was normalized for each joint angle so that $\|\Delta q\|$ was kept smaller than 5°. Essentially, this type of perturbation allows the evaluation of the properties of an equilibrium point: for a stable equilibrium point, the limb will return to its original configuration when subjected to a perturbation.

Joint angles for given perturbation were calculated with inverse kinematic solver in the SIMM softwhere (Musculographics, Inc., Santa Rosa, CA). Due to kinematic redundancy in the closed chain of the hindlimb model, there are multiple solutions that will produce either the same endpoint position or the angle specified at a particular joint. SIMM inverse kinematic solver searches for the solution which results in smallest changes at the joints from the previous posture. Therefore, perturbations were manually controlled to vary gradually for all conditions so that the changes in the joint angles were smooth and continuous function of the perturbation level.

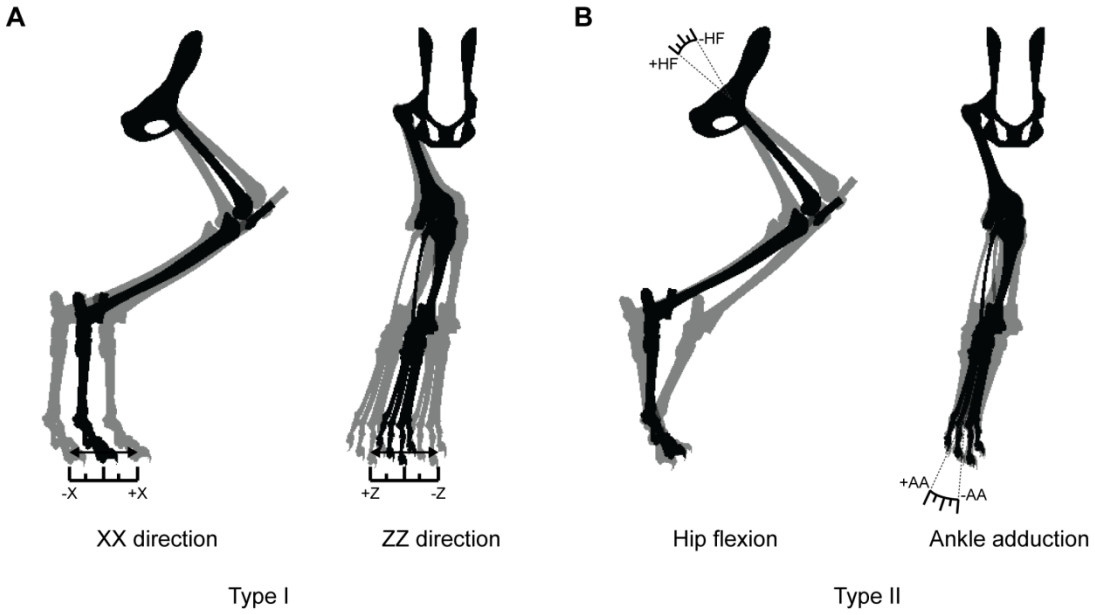

Figure 3. Perturbations applied at the initial joint configuration of the hindlimb model. Black skeletons denote the nominal posture; gray skeletons denote example of perturbed postures. **A:** Type I where the endpoint position was moved from -20 mm to 20 mm in 1 mm increment in four uniformly distributed directions in the horizontal plane. **B:** Type II perturbation where each of the seven joint angles was varied to 20 uniformly intervals while maintaining the endpoint position the same as in the default posture.

In order to assess the dynamic behavior of the system in the presence of perturbation at the joints, forward dynamic simulations were run using custom Matlab (Mathworks, Inc., Natick, MA, USA) routines and NEUROMECHANIC software (www.neuromechanic.com). Five minimum-effort muscle synergies identified from static optimization were used as constant input to the muscles. For simulations performed in this study, variable time step integrator was used with minimum step size of 10E-8. The total simulation time was 1 s where data were acquired for every 1 ms. Dynamic behavior of the system was assessed using the output variables including joint displacement, joint velocity, joint acceleration, moment arm matrices, muscle fiber lengths, endpoint force components, endpoint Jacobian and the linearized state matrix (discussed in detail later). For each of the five minimum-effort synergies simulations were run in 300 different conditions: four directions with 40 steps in Type I and seven joints with 20 steps in Type II.

2.5 Functional stability criteria

In order to assess whether the production of the output force in the model driven by specific muscle activation pattern is functionally stable or unstable, we developed metrics that quantify simulated behavior of a nonlinear biomechanical system in a physiological context. Regarding the timescale where correction can be made with neural delay, as discussed earlier, we consider functional stability as the ability to maintain the joint configuration and the production of the endpoint force vector within range for given time period of the initial 100 ms. Given a detailed biomechanical model, we defined the criteria for functional stability based on the knowledge about the physiological behavior from experimental observations. Briefly, we define the functional stability criteria as;

- Joint angle deviations from the original unperturbed posture must be less than or equal to 5° for initial time period of 100 ms ($\|\Delta q\| \leq 5°$).
- Change in the magnitude of the endpoint force vector must be less than or equal to 20% for initial time period of 100 ms ($0.8 \leq \|F_{End}\| \leq 1.2$).
- Change in the direction of the endpoint force vector must be less than or equal to 10° for initial time period of 100 ms ($\angle F_{End} \leq 10°$).

We defined the time window where any muscle synergy solution should maintain its functional stability to be 100 ms. In the cat experiments, the latency when a force response is elicited following the translational perturbation was about 120 ms (Jacobs and Macpherson, 1996). Therefore, ~100 ms represents the time frame prior to which a correctional neural response could be made for the current state of the dynamics. Electromechanical delay of 100 ms can be attributed to ~40 ms delay of neuromuscular response to be elicited and additional ~60 ms delay for actual force to be generated and transmitted through the musculoskeletal system.

For the criterion regarding the behavior of the kinematic states, we defined configuration changes for functional stability to be within the range where $\|\Delta q\|$ is less than or equal to 5°. During the support surface displacement of 5cm, joint angle changes at the hip, knee and ankle were observed to be within 6° (Ting and Macpherson, 2004). Again, we used $\|\Delta q\|$ as the quantitative measure for overall change in the joint configuration. For the value $\|\Delta q\|$=5°, all of the joint angles could have deviations of 5° respectively or only few joints could have large deviations; deviation at a single joint can be above 10° if there are more than four joints.

We defined the criteria for the endpoint force vector as, when compared to its original force vector, the change in magnitude ($\|F_{End}\|$) should be less than or equal to 20% and the change in direction ($\angle F_{End}$) should be less than equal to 10°. When we examined the total ground reaction force vector during initial passive period of 100 ms, the change in the magnitude and direction were typically less than 10% (observed from data, data not shown here) and 5° (Ting and Macpherson, 2004) respectively. However, it was difficult to discriminate from the total force data the variability associated with the active force. We assumed that the variability would be higher for active force vector because they are generated by activating the muscles in rapid time period during a perturbation and also based on the fact that they are small in magnitude. When producing an active force at the endpoint for postural balance, direction of the force vector is more relevant in terms of producing a consistent behavior. Regarding the force as a three dimensional vector in space, the value 10° gives 1.5% change in the direction of the vector in terms of vector dot product.

2.6 System linearization

In order to test whether linearized system characteristics can predict stability of the five muscle activation patterns, we obtained the state matrices of the system linearized about an equilibrium point at default posture and related its eigenvalues and eigenvectors to the dynamic behavior of the perturbed system. The unique and novel approach of this linearization is that contributions of active muscles to the system dynamics are incorporated, allowing us to test whether characteristics of the unperturbed linearized system could predict the nonlinear behavior of the perturbed simulations. The linearized system state matrix describes how a small change in each of the states will affect the system by linearly approximating the local dynamics of the entire nonlinear

musculoskeletal model around an equilibrium point. The eigenvectors of the state matrix represent the basis vectors that span all possible variations (modes) that can be made on the system. The corresponding eigenvalues determine how the system responds to such modes and determines system's Lyapunov stability.

The state matrix for a system defined with the kinematic states $\vec{q}$ and $\dot{\vec{q}}$, muscle force generated with the specified muscle activation and resulting reaction force at the can be given as follows. From the equations of motion (Eq. 1),

$$\ddot{\vec{q}} = f = \mathbf{M}^{-1}(\mathbf{R}\vec{F}_M - \mathbf{J}^{\mathbf{T}}\vec{F}_{End} - \vec{V}) \tag{4.1}$$

We obtain the linearized system state matrix about an equilibrium point using the Taylor-series expansion to the first-order. At an equilibrium point, the system is balanced to all external forces and moments and there are no changes in the states with respect to time: $f = \mathbf{0}$. Therefore,

$$\begin{bmatrix} \Delta\dot{\vec{q}} \\ \Delta\ddot{\vec{q}} \end{bmatrix} = \mathbf{A}\begin{bmatrix} \Delta\vec{q} \\ \Delta\dot{\vec{q}} \end{bmatrix} \text{ where the state matrix, } \mathbf{A} = \begin{bmatrix} \mathbf{0} & \mathbf{I} \\ \dfrac{\partial f}{\partial \vec{q}} & \dfrac{\partial f}{\partial \dot{\vec{q}}} \end{bmatrix} \tag{4.2}$$

Mathematically, it is the Jacobian matrix with respect to the system states. NEUROMECHANIC computes the state matrix by numerically perturbing each of the states at a specified difference for each of the states. For the results reported in this study, difference of 10E-8 was used for precision. However, it was found that using 10E-3 did not make significant difference in the resulting state matrix: RMS error between the two matrices was 2.24E-5%.

We evaluated the Lyapunov stability of the five muscle activation patterns by calculating the eigenvalues. Further, we test whether the dynamic behavior of the perturbed system can be predicted with the linearized system characteristic by relating the behaviors to the sign and magnitude of the eigenvalues in terms of doubling time (Eq. 5), and also by matching the changes in the kinematic states to the eigenvectors.

$$t_{double} \equiv \frac{\ln(2)}{\mathrm{Re}(eig)} \tag{5}$$

CHAPTER 3

RESULTS

3.1 Minimum-effort muscle synergies

Identified muscle activation spanned multiple joints for all minimum-effort muscle synergies.

Muscle recruitment within the identified muscle activation patterns (W1~W5) using minimum-effort as the cost function fulfilled the joint torque requirement for each of the five synergy force vectors SFV1~SFV5 (Fig. 4). Given a configuration of the limb, torque required at each of the DoFs is uniquely determined by the specified endpoint force. For example, SFV1 was produced mostly by knee extension and hip flexion where the force vector pushes against the ground in back and outward direction. On the other hand, SFV2 which is a force vector that pulls up the limb in inward direction was produced by knee and hip flexion. In addition, SFV3 and SFV4 had large horizontal (shear) force component relative to the vertical component. For all five synergy force vectors, most significant torque was required at hip flexion/extension (±HF) or knee extension/flexion (±KE). All minimum-effort muscle synergies had activation of muscles mostly in the hip and knee where W3 and W4 had activations in the ankle muscles as well. Minimum-effort solutions showed some agreement with the experimentally identified muscle synergies such as relatively high activation for the VL which mostly acts for the knee extension and recruitment of the flexors such as PSOAS and TA in W2. Compared to other synergies, W3 had relatively large co-activation of various muscles spanning most of the DoFs.

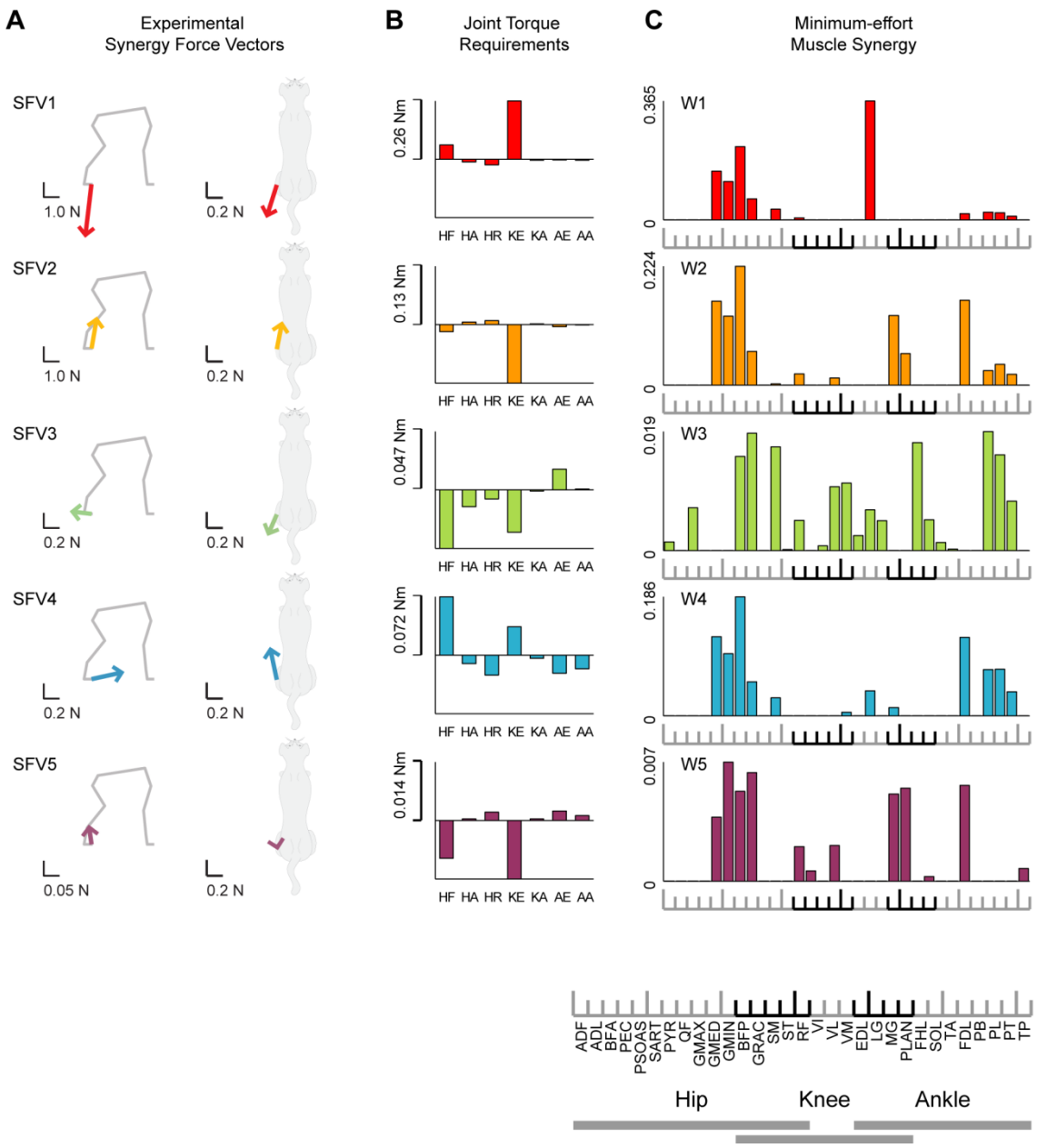

Figure 4. A: Five muscle synergy force vectors, **B:** resulting torque required at the joints and **C:** identified muscle activation patterns for minimum-effort muscle synergies. Muscle recruitment within minimum-effort muscle synergies were in agreement with the joint torque requirements specified by each of the synergy force vectors. SFV1 was produced by knee extensors and hip flexors in W1 whereas SFV2 was produced by both knee and hip flexors in W2. Muscles labeled with darker ticks are those that span both hip and knee or knee and ankle.

To meet the torque requirement over all seven DoFs in the model, antagonistic muscle were co-activated even when the criteria was to minimize muscle activation. Muscles have moment arms about multiple DoFs. The muscle activations that meet the requirement at a set of joint torques can be visualized in vector space (Valero-Cuevas, 2009). When W1~W5 were observed in the torque space, muscles recruited in the solution included those that act antagonistically to the required torque in four of the five synergies. For example, QF in W1 was activated even when the torque generated by QF was almost opposite to the torque required at hip flexion and hip rotation was activated (Fig. 5A). In W2, PSOAS and PYR were activated which had actions at the hip opposite to the required torque (Fig. 5B). Similarly, PYR, RF and VL in W3 and PSOAS in W5 were acting opposed to the required torque. It was also shown in the torque space that the solutions differed in how muscle recruitment met the torque requirement. For example, ankle torque in W1 was generated mostly with co-activation of muscles with similar moment arms at a given DoF, whereas in W2, we observed co-activation of muscles with opposite moment arms about the ankle. Muscles that appear to be antagonists to the desired torque and nonetheless activated necessary to meet three dimensional torque requirements (Aithaddou et al., 2004; Jinha et al., 2006).

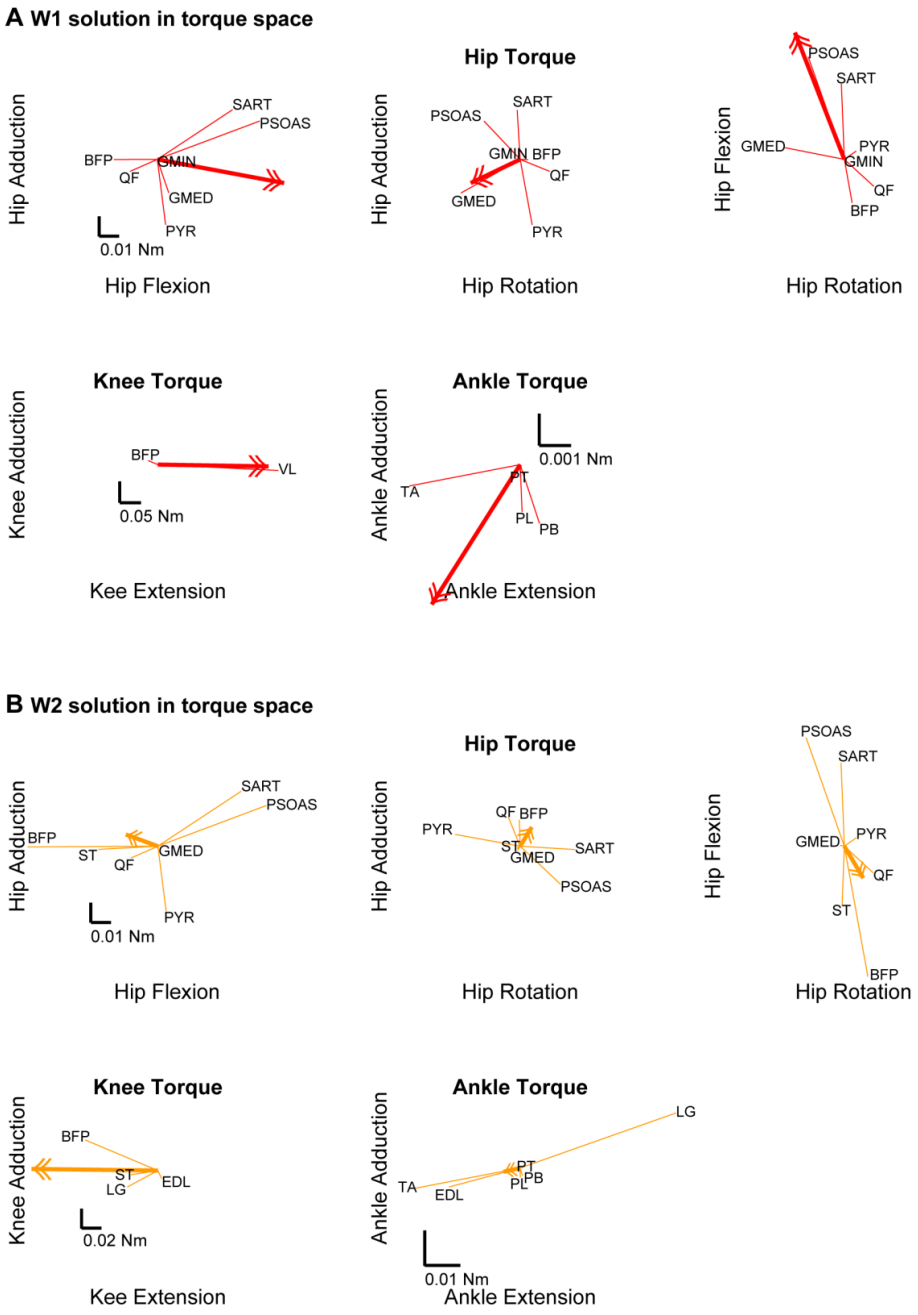

Figure 5. Minimum-effort muscle activation pattern for W1 (**A**) and W2 (**B**) observed in torque space. Thick lines indicate net torque vector generated. Thin lines denote torque contributions of each muscle contributing to the torques. Muscles that are antagonistic to the torque requirement are recruited to meet the overall torque requirement in the seven DoFs: QF in W1 and PSOAS and PYR in W2. Also note that the ankle torque in each W1 and W2 is produced by muscles that have respectively similar and opposite moment arm action about given DoF.

3.2 Functional stability assessment

Four of five minimum-effort solutions satisfy functional stability criteria.

All minimum-effort muscle synergies except W1 were functional stable when all of the data points for $\|\Delta q\|$, $\|F_{End}\|$ and $\angle F_{End}$ were evaluated at 100 ms and applied to the functional stability criteria (Table 2). In order to examine the overall trend at 100 ms with respect to time, data points were also evaluated at the 0 ms and 200 ms time point (Fig. 6). W1 had about 30% of the conditions outside the range for functional stability in all three criteria increasing with significant rate (slope in Fig. 6). W2, W4 and W5 satisfied all of the criteria in all conditions. W3 also satisfied all of the criteria in most of the conditions. In W3, there were few conditions where certain criterion was violated to a small degree: $\|F_{End}\|$ in five conditions (5/300) were below 80% at 75.0%, 76.5%, 77.9%, 79.4% and 79.5% each. However, W3 was not considered functionally unstable because differences to the threshold were subtle at these points and were decreasing when $\|\Delta q\|$, $\|F_{End}\|$ and $\angle F_{End}$ were evaluated at 200ms.

Table 2. Assessing functional stability of five minimum-effort muscle synergies

	$\|\Delta q\| \le 5°$		$0.8 \le \|F_{End}\| \le 1.2$		$\angle F_{End} \le 10°$		t_{double} (ms)
W1	**4.95 (5.47)**	**98/300**	**0.86 (0.21)**	**80/300**	**8.88 (17.5)**	**82/300**	**33.16, 47.78**
W2	1.39 (0.91)	•	1.00 (0.01)	•	2.24 (2.16)	•	-303.8
W3	1.41 (0.87)	•	0.99 (0.06)	5/300	2.09 (1.60)	•	**210.6**
W4	1.45 (0.88)	•	1.00 (0.03)	•	2.08 (1.94)	•	-548.4
W5	1.62 (1.04)	•	1.00 (0.03)	•	2.37 (1.92)	•	**430.6**

Values show mean (std) and number of data point that did not satisfy the criteria. Case when all data points were within the criteria is indicated with •. Maximum t_{double} is also reported where negative value indicates eigenvalue with positive real part. Values in bold are those determined unstable by functional stability or Lyapnov stability.

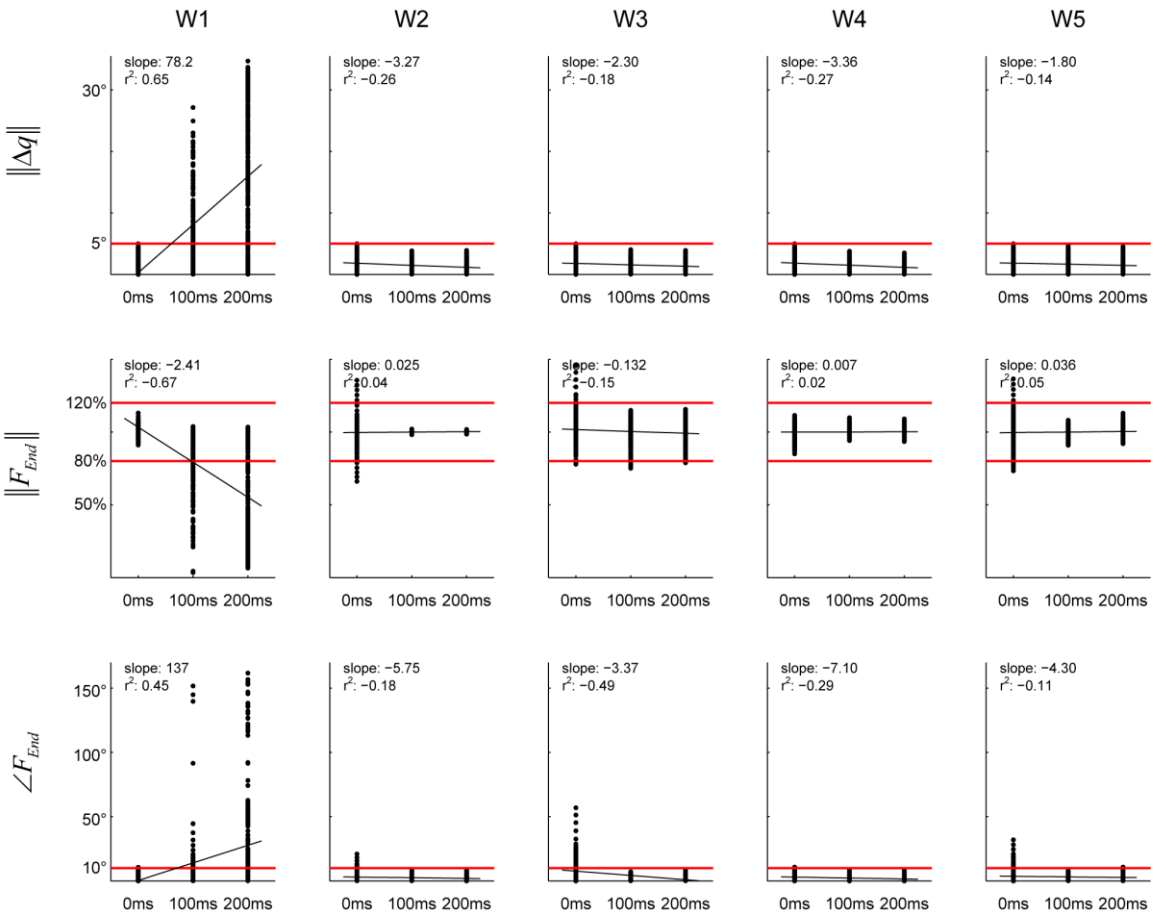

Figure 6. Data points of $\|\Delta q\|$, $\|F_{End}\|$ and $\angle F_{End}$ in all 300 conditions for W1~W5 evaluated at 0 ms, 100 ms and 200 ms. Red lines indicate criteria for functional stability at 100 ms. Slope of the fitted line shows the general trend over initial 200 ms where the intersecting point with the data points distributed in vertical represents the mean value for 300 data points.

Because the moment arms and endpoint Jacobian for a given perturbation is same for all synergies, variation in the initial $\|\Delta q\|$ is consistent across all synergies. For the output force vector, it is shown that variations at the initial time point were different across synergies. In particular, W1 was most insensitive whereas W3 and W5 had relatively large variations (Fig. 6) in terms of the force direction, which is important in postural control because active force generation is to induce change in the total reaction force against the ground. In order to further investigate which feature of each synergy attributed to this relationship, we further looked at the characteristics of the muscles of which the synergy is composed of. For a given perturbation, difference in sensitivity of each muscle synergy to the perturbation is related to fiber length changes among the muscles recruited within the synergy. When range of the change in the fiber length of each muscle due to each perturbation was measured across all conditions, it showed that some muscles such as GMED and GMIN had large range for all perturbation whereas some muscles such as FHL, SOL and TA had almost no changes for any of the perturbation (Fig. 7).

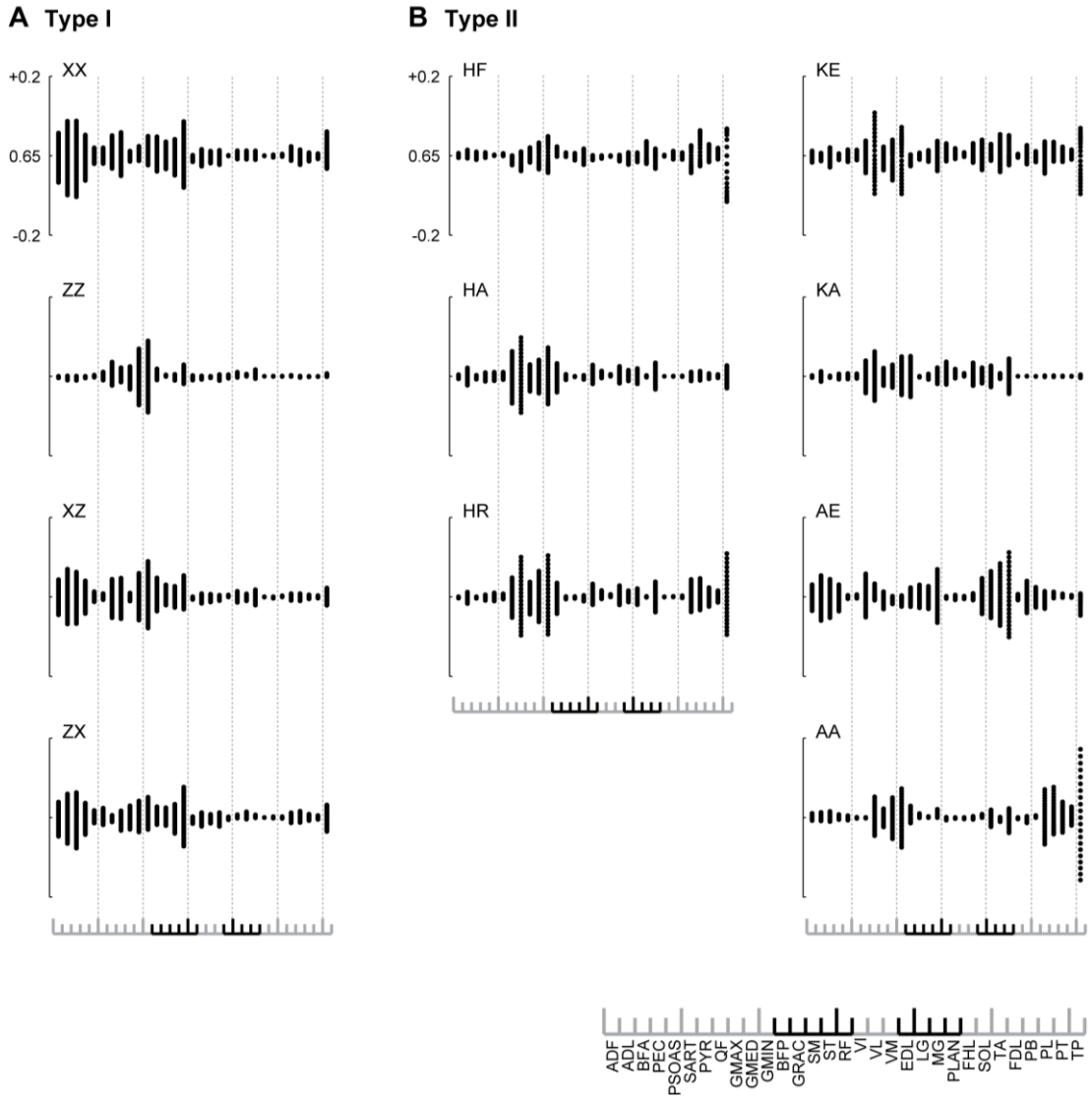

Figure 7. Range of muscle fiber length changes in each type of perturbations. Muscles show various sensitivity in muscle fiber length changes due to perturbation. All muscles are set to have normalized fiber length of 65% at default posture.

When muscle activation vector (Fig. 4C) was mapped to this fiber length range vector by calculating the dot product of the two vectors normalized to its own magnitude, it showed that W1 was most insensitive where as W3 and W5 were sensitive to perturbation (Table 3). The fact that any particular muscle activation pattern may exhibit characteristic sensitivity to the perturbation in terms of endpoint force generation implies that joint configuration and output force cannot necessarily replace one another but rather both should be included in the criteria for assessing functional stability. Moreover, it also leaves the possibility that recruiting the muscles that are insensitive to postural variation in terms of fiber length changes may be beneficial for consistent production of the output (see DISCUSSION).

Table 3. Sensitivity of the five minimum-effort muscle synergies to the muscle fiber length changes resulting from given perturbations.

	Type I				Type II						
	XX	ZZ	XZ	ZX	HF	HA	HR	KE	KA	AE	AA
W1	0.21	0.10	0.19	0.12	0.07	0.22	0.21	0.20	0.15	0.14	0.08
W2	0.31	0.15	0.28	0.16	0.16	0.38	0.36	0.41	0.28	0.41	0.15
W3	**0.78**	0.41	**0.72**	**0.57**	**0.57**	**0.74**	**0.93**	**1.00**	**0.58**	**0.76**	**0.69**
W4	0.31	0.17	0.28	0.17	0.19	0.37	0.39	0.38	0.23	0.28	0.22
W5	**0.51**	0.22	0.43	0.30	0.25	**0.58**	**0.59**	**0.68**	0.47	**0.61**	0.30

Sensitivity is defined as the dot product of the solution vector and the fiber length range for given perturbations, normalized to the maximum value across all conditions. Numbers in bold are those that have the value greater than 0.5.

3.3 Prediction with linearized system characteristics

Eigenvalues of the linearized system can predict functional stability and classify the behavior of muscle activation pattern with respect to time.

Overall behavior of the criteria were in correspondence with the doubling time (t_{double} , see METHODS) of the dominant eigenvalue of the linearized system. When behaviors of the three variables $\|\Delta q\|$, $\|F_{End}\|$ and $\angle F_{End}$ were observed over the whole time course of the simulation (Fig. 8), W1 which had two eigenvalues that had positive real parts of 14.5 and 20.9 corresponding to t_{50} of 33.2 ms and 47.8 ms, respectively, showed fast deviating behavior within 100 ms. W3 and W5 each had one eigenvalue with positive real part of 3.29 and 1.61, respectively. In correspondence with t_{double} of 210.6 ms and 430.6 ms, W3 and W5 only deviated above the range for functional stability approximately after 500 ms and 1 s, respectively. W2 and W4 which had no eigenvalues with positive real part stayed within the range for most of the time period. However, W4 showed deviating behavior after 500 ms in few perturbation conditions.

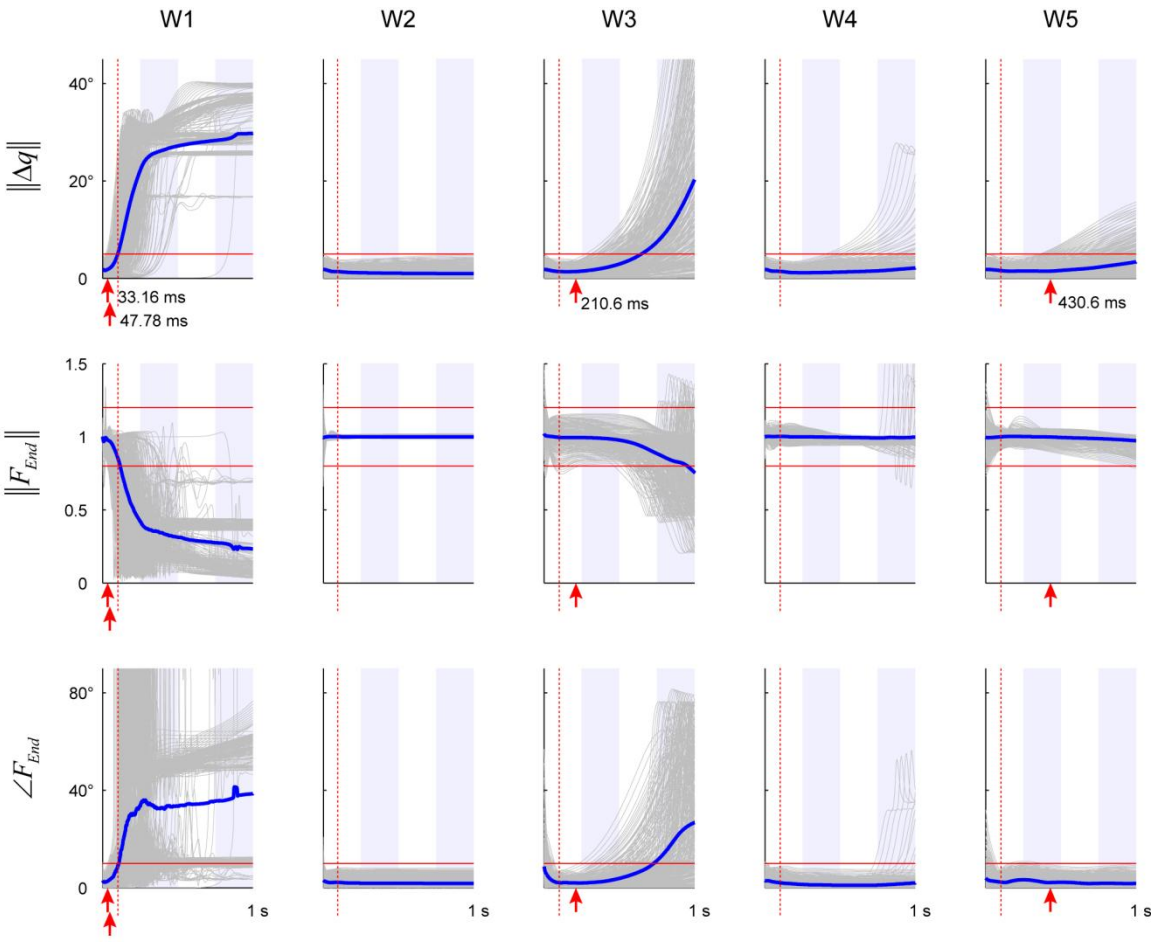

Figure 8. Time traces of the three variables in functional stability criteria $\|\Delta q\|$, $\|F_{End}\|$ and $\angle F_{End}$ for W1~W5 over total time period of simulation (1s, shaded area is each 250 ms). Bold trace is the mean across all perturbed conditions in each synergy and gray are the actual traces for each condition. Vertical line indicates the 100 ms time point where functional stability of a muscle activation pattern is evaluated and red horizontal lines indicates the range for each of the functional stability criteria. Red arrows indicate doubling time (t_{double}) of positive eigenvalues.

Dynamic behavior of the kinematic states in each minimum-effort muscle synergy had characteristic modes of how individual joints change.

In general, trend in the evolution of the joint kinematic states over time was consistent within synergy and type of perturbation, where the rate of response was proportional to magnitude of the overall level of muscle activation and the level of perturbation. However, behavior of the kinematic states observed during the overall time course of the simulation differed across both synergy and perturbation type. In order to examine the extent to which behavior was distributed across joints, we further examined the dynamic behavior of the individual kinematic states.

In particular, deviations of the joint angles in unstable W1 were most considerable at the ankle extension and ankle adduction (typical example in Fig. 9) which increased at rates typically greater than hundreds of °/s within 100 ms. For most conditions with high level of perturbation, joint angle deviation at the knee and ankle within 100 ms exceeded 10° and 20° respectively. The behavior that shows fast increase at the ankle followed by gradually increased hip rotation was similar across both the type and the level of perturbation. Within the total time of the simulation, 1 second, posture of the limb converged to a non-physiological configuration with hyper-extended knee and ankle where it appeared to be rotated inside out as the motion stops.

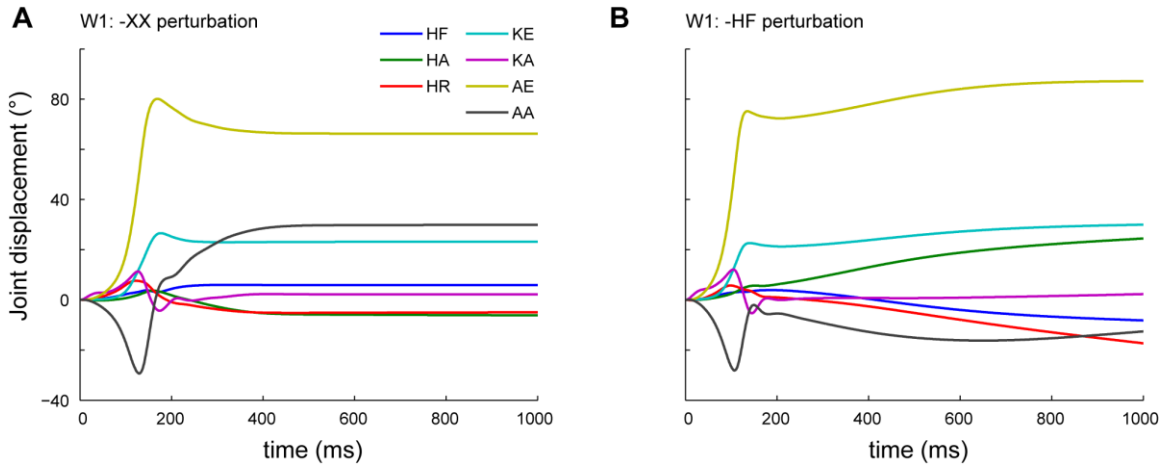

Figure 9. Time traces of joint displacements in W1 for **A:** perturbation Type I at maximum –XX condition and **B:** perturbation Type II at maximum +HF condition. Deviations of the joint angles in unstable W1 were most considerable at the AE and AA then HR. Bold flat and dashed lines indicate averaged trace for positive and negative direction in each perturbation respectively.

In W3 (Fig. 10A and 10B) which was stable within 100 ms, joint configuration was typically converging to initial posture for first 200 ms where joint deviations were less than 10° and decreasing. After about 500 ms, it started to have similar growing phenomenon where most significant deviations were at HA and AE. Similarly, in W5 (Fig. 10C and 10D), joint deviations were small for most of the conditions: less than 5° within 100 ms and less than 10° within total time of simulation. However, joints were slowly diverging with velocity less than 20°/s in perturbation Type I and most of the conditions in perturbation Type II. Most significant deviations were at HA, KA and AA.

In W2 and W4 which were stable, change in individual joint angle within 100 ms stayed less than 10° for all of the conditions for W2 (Fig. 11A and 11B) and W4 (Fig. 11C and 11D). Joint velocities developed within 100 ms were mostly large at KA, AE and AA. However, in perturbation Type I, it was found in W4 that the limb was gradually diverging from the stable posture when the position of the toe was perturbed in backward direction. When perturbation level was higher than 10 mm, it showed unstable behavior which was similar to W1. For perturbation Type II, the limb posture was always converging to a stable posture in both W2 and W4.

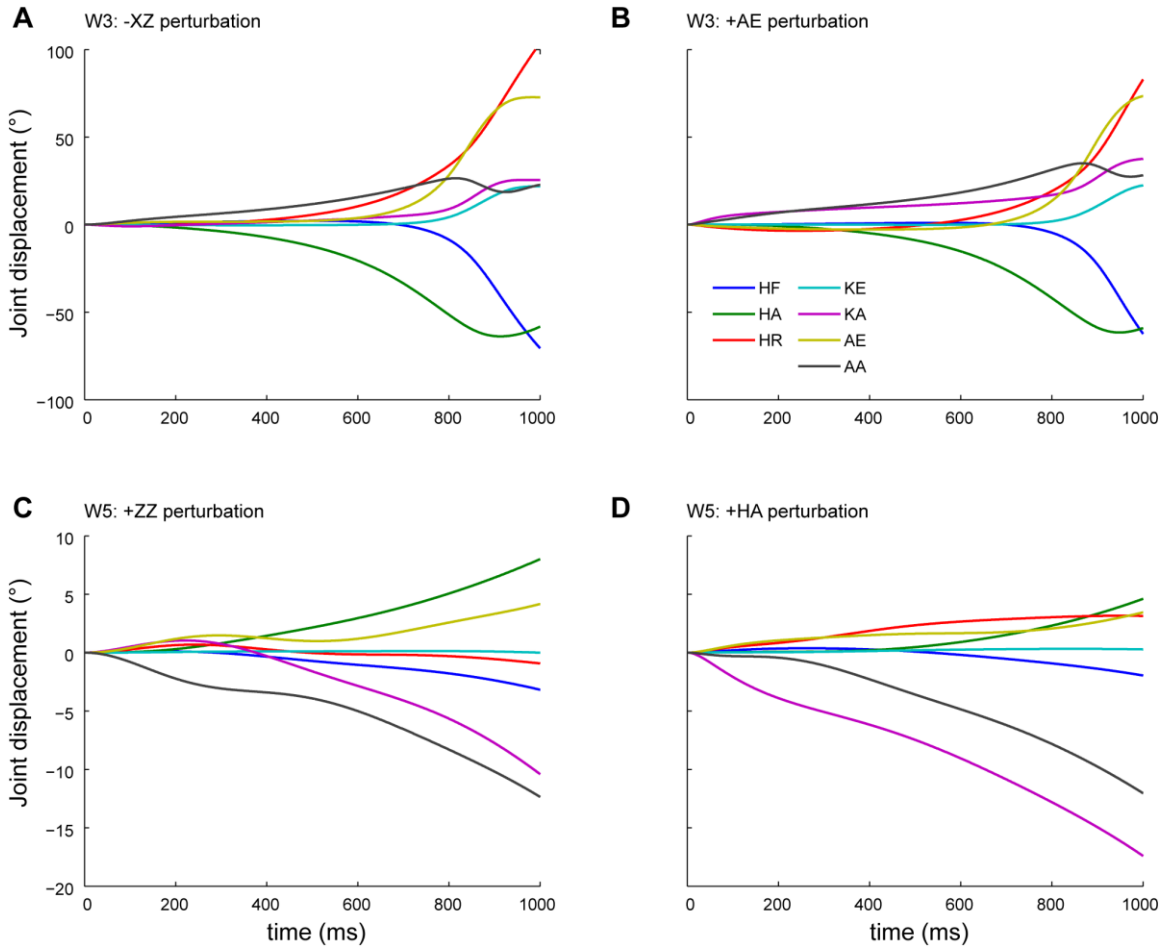

Figure 10. Time traces of joint displacements in W3 and W5. **A:** W3 in perturbation Type I at maximum –XZ condition. **B:** W3 in perturbation Type II at maximum +AE condition. **C:** W5 in perturbation Type I at maximum +ZZ condition. **D:** W5 in perturbation Type II at maximum +HA condition. Deviations of the joint angles were most considerable at HR and AE in W3 and at in HA, KA and AA in W5.

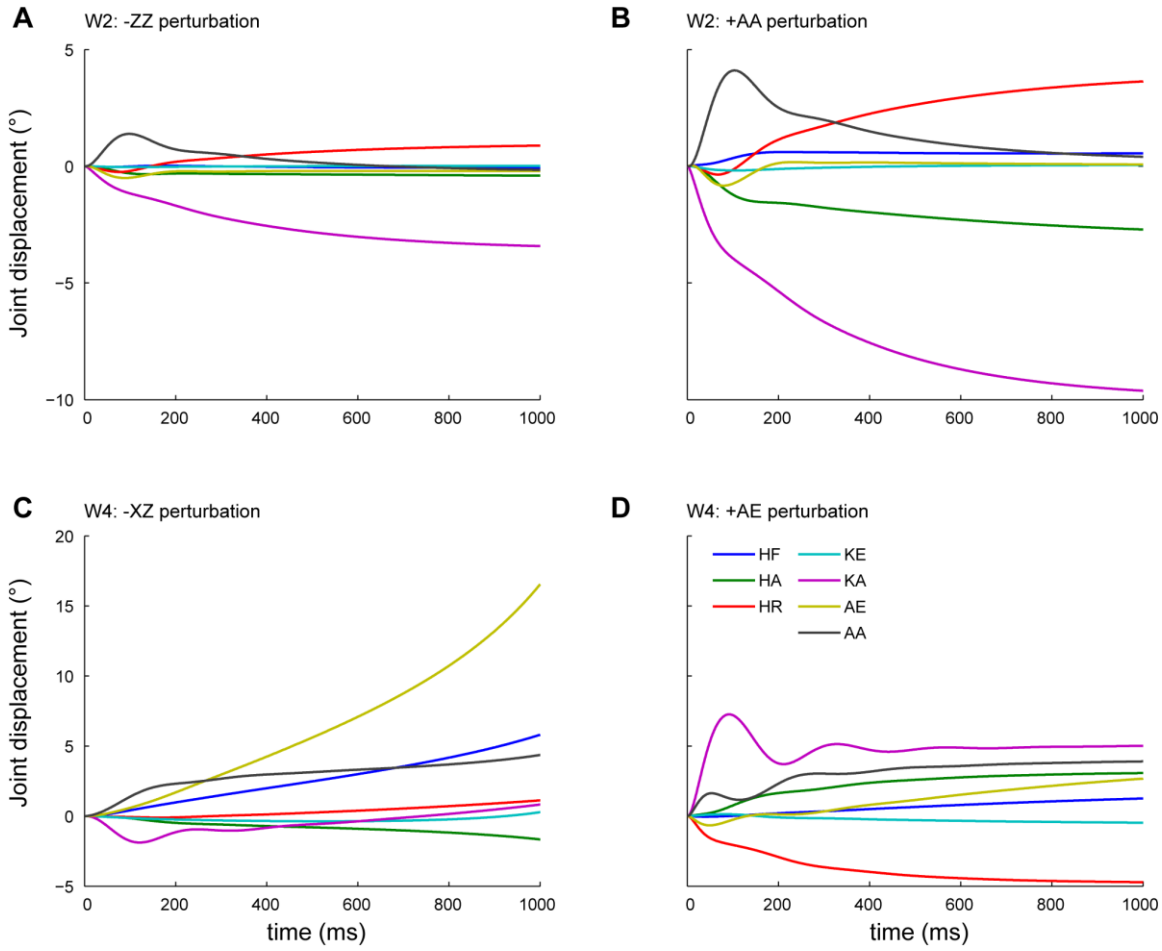

Figure 11. Time traces of joint displacements in W2 and W4. **A:** W2 in perturbation Type I at maximum –ZZ condition. **B:** W2 in perturbation Type II at maximum +AA condition. **C:** W4 in perturbation Type I at maximum -XZ condition. **D:** W4 in perturbation Type II at maximum +AE condition. W2 and W4 showed converging behavior in most of the conditions where W4 had diverging behavior similar to W1 when the limb endpoint was perturbed in backward direction at a level higher than 10mm (C).

Eigenvectors of the linearized system can explain the joint kinematic behavior at given time corresponding to its eigenvalue

In all minimum-effort muscle synergies, dynamic behavior of the unperturbed system could be explained with the eigenvectors of the linearized system that are in particular related to velocity-state. For all five synergies, there were eight eigenvectors with significant components corresponding to joint velocity states and six that had large components at joint displacement states. However, eigenvalues of displacement-state eigenvectors were significantly smaller in magnitude for all synergies, in the order of ~10E-5 whereas velocity-state eigenvectors had eigenvalues from ~1 to ~100 which corresponds to the response time in the scales of ~10 ms to ~1 s. Therefore, dynamic behavior of the perturbed system was considered to be dominated by one or more of the velocity-state eigenvectors (Fig. 12).

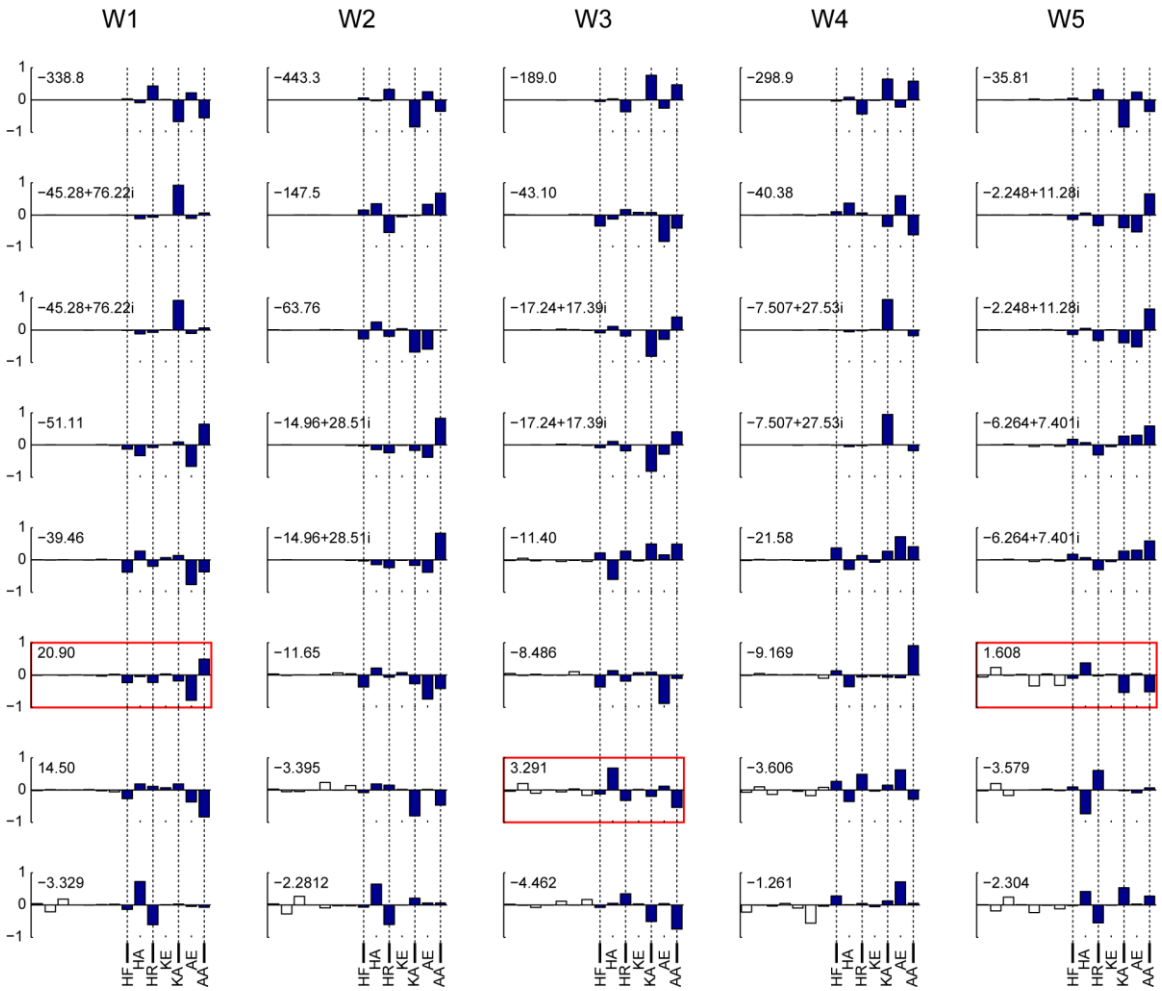

Figure 12. Eight velocity-state eigenvectors for minimum-effort muscle synergies. Numbers in each of the bar pots are the corresponding eigenvalues of each eigenvector. Filled bars indicate components related to joint velocity states at HF, HA, HR, KE, KA, AE and AA eachs. Boxed are the eigenvectors that had positive real part in its eigenvalue.

In order to quantify which eigenvector was dominating the behavior at given time, we matched all eight eigenvectors to the joint velocities developed at each time point by calculating the dot product of the two vectors normalized to its own magnitude. Resulting value of this dot product is between 0 and 1 where the value 1 indicates that joint velocities developed at given time perfectly match with a specific eigenvector. When value 0.95 was considered as a significant correlation, the results showed that one or more eigenvectors were driving the system time corresponding to the eigenvalue, or the doubling time. In particular, the system was driven by the unstable modes at time corresponding to the doubling time for each eigenvector which could discriminate whether a muscle activation pattern is functionally stable or unstable (Fig. 13): W1 had two eigenvectors that had t_{double} less than 100ms. W1 was functionally unstable; W3 and W5 each had one eigenvector with t_{double} of 210.6 ms and 430.6 ms. These eigenvector were dominating the behavior approximately after 200 ms and 400 ms each in W3 and W5. Therefore, W3 and W5 were functionally stable.

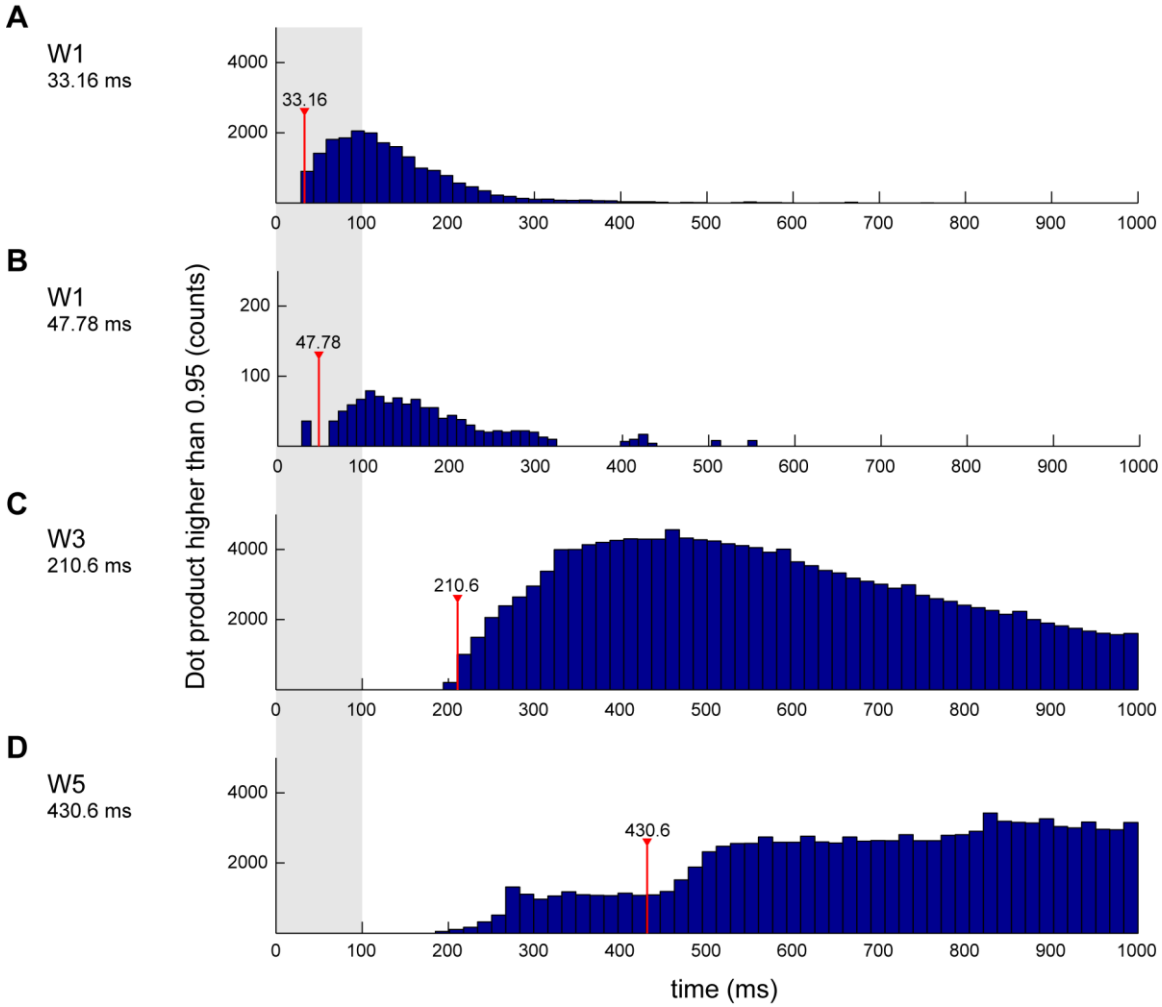

Figure 13. Histogram of the time points where joint velocities at given time point matched the eigenvectors (dot product higher than 0.95) with positive eigenvalues in W1, W3 and W5. **A** and **B:** W1 was functionally unstable with two eigenvectors with t_{double} of 33.16 ms (A) and 41.76 ms (B) which was dominating the unstable behavior within 100ms. **C** and **D**: W3 and W5 each had one eigenvector with t_{double} of 210.6 ms (C) and 430.6 ms (D). These eigenvector were dominating the behavior approximately after 200 ms and 400 ms each in W3 and W5. Therefore, W3 and W5 were functionally stable.

Eigenvalues are scaled monotonically as a function of the synergy activation level.

Since magnitude of the eigenvalue determined the time where muscle activation pattern turns functionally unstable, we investigated how activation level of each muscle synergy affected the magnitude of the eigenvalues. When activation level was scaled from x0.1 to x2.0 for each muscle synergy, eigenvalues seemed to spread out from the origin as activation level increases (Fig. 14A). Minimum real parts of the eigenvalues were largely negative for all synergies and increased in magnitude as activation level increases. For minimum real part of the eigenvalues, positive eigenvalues in W1, W3 and W5 increased in magnitude varying approximately about from 45% to 120% with increasing activation level. Negative, but still with maximum real part, eigenvalues in W2 and W4 decreased in magnitude from 120% to 98% with asymptotic convergence. However, there were no sign changes in any of the maximum eigenvalues (Fig. 14 B).

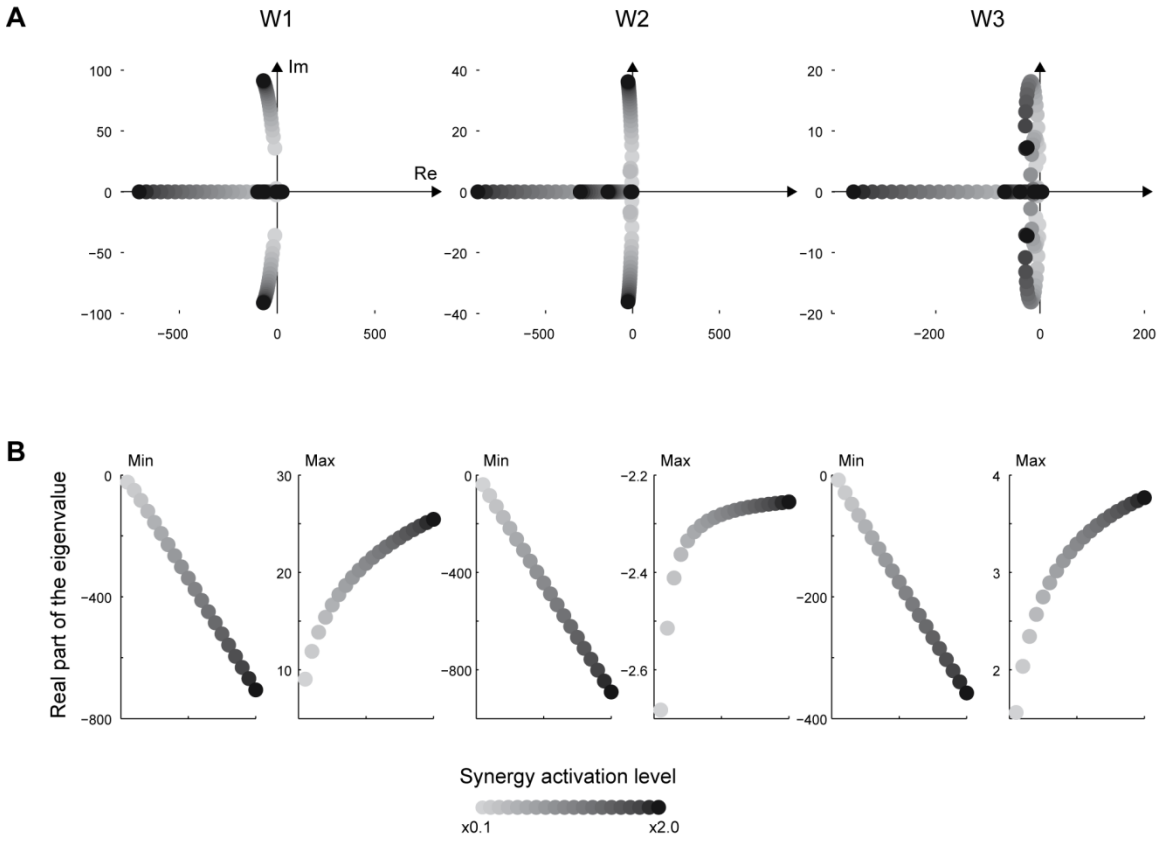

Figure 14. Scaling of eigenvalues as a function of muscle synergy activation level. **A:** Eigenvalues that correspond to velocity-state eigenvectors of W1, W2 and W3 in complex plane at various activation level (darker the higher). **B:** Minimum and maximum real part of the eigenvalues for velocity-related eigenvectors of W1, W2 and W3 as a function of activation level. As activation level increases, eigenvalues tend to spread out from the origin: positive ones go more positive and negative ones go more negative.

The level of muscle activation could affect the dynamic response where high activation may result in faster rate of response to any change to the system. However, it was actually found that the magnitude of the synergy force vectors and resulting activation level of each identified muscle synergies had consistent relationship to the magnitude of the unstable eigenvalues W1 (20.9) > W3 (3.29) > W5 (1.61). In this study, no normalization was made either on the experimental synergy force vectors or the identified muscle synergies because the magnitude of the force and thus the level of muscle activation within muscle synergies may be the inherent nature of the given solution. However, it was found that scaling the magnitude of the force does not affect the solution in term of the composition but just scales the level of activation of the same muscle coordination (result not reported here). Moreover, varying the magnitude of the activation level for given muscle activation pattern scaled the magnitude of the eigenvalue with asymptotic limit but did not change the sign of eigenvalue. Therefore, it can be concluded that mathematical stability of the linearized system is independent of the magnitude of the output force and thus the level of activation, whereas it may be functionally stable or unstable depending on the level of activation.

CHAPTER 4

DISCUSSION

The primary result of this work was to demonstrate that minimum-effort muscle synergies obtained from static models may provide functionally stable dynamic behavior in some, but not all cases, with the implication that functional stability criteria should be considered in musculoskeletal modeling studies.

4.1 Assessing stability of muscle activation patterns

Minimum-effort muscle synergies can be functionally stable or unstable in dynamic contexts. Four of five muscle activation patterns that produce each of the five synergy force vectors with least amount of muscle activity were found functionally stable. This was surprising regarding the complexity of the model, which is even more difficult to be stabilized or even analyzed when actuated with muscles that have nonlinear characteristics. Regarding biological systems including musculoskeletal systems, the very definition of stability has always been controversial (Hasan, 2005). Given a muscle activation pattern and certain range of behavior, stability of the whole system can depend on many things. The magnitudes of the output force vectors determines the overall levels of muscle activation in each identified muscle pattern and therefore affects the rate of the dynamic response. Also, owing to the differences in muscle fiber lengthening properties of each muscle in each direction of perturbation, muscle recruitment within a given solution affects both the magnitude and direction of the output force vector when system is perturbed. In order to encapsulate all features that contributed to overall stability of the system, we used empirical criteria describing the behavior of producing a specified endpoint force. Wide variety of physiologically relevant perturbations, particularly within the paradigm of postural control, was given to the system and resulting behavior was

assessed with excessive amount of data generated from simulation. The result showed that the specified criteria are effective in terms of discriminating functionally stable or unstable behavior.

In the context of detailed musculoskeletal modeling, linearized system characteristics may provide important information about the dynamic behavior of the nonlinear system. Interestingly, eigenvalues and eigenvectors of the linearized system were able to predict various aspect of the functional behavior in a full dynamic, nonlinear system. Although system linearization about an equilibrium point in non-linear systems provides substantial information about the local behavior, it has not been applied to any realistic musculoskeletal models and demonstrated that whether or to what extent the linearized system characteristics could predict the behavior of the biomechanical system. This approach, enabled by the NEUROMECHANIC software, was a novel method of utilizing a detailed biomechanical model to evaluate stability of a muscle activation pattern while incorporating the intrinsic properties of active muscles. Important implication lies in modeling studies in neural control of movement where prior knowledge on how particular muscle activation pattern would function in dynamic aspects for certain range of behavior, certain time frame of interest, may provide more insights before any further extensive investigation should be done in an exploratory manner.

4.2 The minimum-effort criteria

Taken together with previous experimental studies, our results suggest that the nervous system must be considering criteria in addition to minimizing effort - such as maximizing stability - as the criteria for selecting muscle activation patterns in postural control. In balance control of cats, there is no functional response or changes in muscle activity during initial 100 ms following the onset of perturbation. Nevertheless,

background force vector that is used constantly in quiet standing is capable of maintaining the joint configurations within certain range for this time period in which the nervous system cannot respond. In our previous study, one of the five experimentally identified muscle synergies, W1, was found to produce the background synergy force vector which is used both in quiet stance and during perturbation (Ting and Macpherson, 2005; Torres-Oviedo et al., 2006). Based on our knowledge from experimental observation, it is evident that the biological muscle activation pattern for W1 must meet the criteria for functional stability established in this study. However, our results showed that W1, when muscle activation pattern was predicted using minimum-effort criterion, did not satisfy the functional stability criteria whereas other four minimum-effort muscle synergies were functionally stable. Therefore, minimum-effort is not a sufficient criterion for choosing muscle activation pattern in postural control.

Specifically considering W1, we speculate that additional co-activation is required at the ankle because W1 had relatively small activation at ankle muscle whereas in experiment ankle muscles such as SOL were obviously recruited. Simulations showed that most unstable deviations in W1 were at the ankle joint which was also in agreement with the dominant unstable eigenvector having most considerable velocity components at the ankle extension and adduction. Moreover, it has been demonstrated with the same hindlimb model studied here that muscle activation pattern generating the stance-like force can be stabilized when increased co-activation based on heterogenic length feedback from other muscles were included (Bunderson et al., 2010). Four muscle synergies that were functionally stable are thought to be activated solely to induce change in the endpoint force in order to make corrections to the total force and moment at the center of mass to maintain balance. Minimum-effort solutions may be sufficient in this case where recruitment of theses muscle synergies are limited in short time period, 80ms window. However, if muscle synergies are to be activated continuously for a longer time period such as in walking, sustaining external loads or even when subjected to a

continuous perturbation, minimum-effort solutions in this case may also fail to provide functional stability.

Results from other motor tasks also suggest that the nervous system does not select muscle activation pattern solely based on energetic efficiency, instead opting to use additional co-contraction to satisfy additional task criteria. It is further supported by experimental evidence in arm reaching tasks where increased co-activations of muscles were observed in performing a reaching task in an unstable environment which suggests that additional co-contraction might be required instead of using energetically most efficient solution (Franklin et al,. 2008, Kistemaker et al., 2010). Other experimental studies in human walking also suggest that subjects may trade off effort expenditure for stability during motor tasks (Hunter et al., 2010). There also are studies that showed minimizing effort only failed to predict behavior in arm movements, eye movements (Nelson, 1983; Harwood et al., 1999). Moreover, in certain motor tasks where the goal is to maximize performance such as in pedaling (Raasch, 1997), the task itself requires different aspects other than energetic efficiency to be considered. Nevertheless, there still are evidences and reasons that solution for a repetitive or persisting movement may converge to the one that has less, or least, effort expenditure (Hoyt and Taylor, 1981; Alexander, 1989 and 2005). Therefore, the choice of the nervous system for given task should be a good enough, but not necessarily the best for one case, solution derived from the trade-off between multiple cost functions in the context of the task requirement as suggested by others (Todorov, 2004; Ganesh et al., 2010).

4.3 Practical requirements for stable solutions

Our results suggest that assessing the stability of motor solutions, not just energetic cost may also be useful to produce biomechanical simulations that are intrinsically stable and therefore insensitive to sources of instability such as numerical

round-off error. In two dimensional stable tasks or in a simple model, the minimum-effort solution may be sufficient to function or reproduce the behavior in the model. However, if the model is subjected to more challenging conditions in three dimensions or in the presence of perturbations or noise, as is always the case for biological systems, minimum-effort solutions may be insufficient to provide stability. One current numerical simulation package (OpenSim, Delp et al., 2007) which uses computed muscle control (CMC) algorithm to obtain muscle activation pattern that generates motion that tracks prescribed data (Thelen et al., 2003) reports the problem of deviation from the desired trajectory within less than 40 ms, the delay of muscle excitation to actual force generation, and accumulation of error which needs to be fixed with an ad-hoc methods (Thelen and Anderson, 2006). It is unlikely that muscle patterns chosen by the nervous system would lead to such instability, because responding to instabilities within a small time period would be impossible for the nervous system, which is limited to response latencies of 40 ms or more due to neural transmission and processing delays. However, it may help solve this problem if a solution is capable of handling the deviation that leads to unstable simulations over certain range of time, using intrinsic stabilizing properties of active muscles. Essentially, we can test if a solution in the simulation will behave functionally stable or not in the context of the given task. We propose some general idea how to stabilize a muscle activation pattern which we discuss later.

4.4 Implications in postural muscle synergy

We speculate that muscle synergy patterns selected by the nervous system to provide functional stability may allow the nervous system to use a linearized internal representation of the complex biomechanical system. Clearly, the mapping from muscle activation via the biomechanics and configuration to the output force can be an explicit function of the joint states defined through moment arms, active force-length curve and

endpoint Jacobian. However, because the joint states are inter-coupled and the relationships are highly nonlinear, it is difficult that the change in the production of the endpoint force can be attributed to change in muscle activation linearly. Nevertheless, it is surprising that the nervous system may use a control scheme of linearly combining a few set of basis input vectors, the muscle synergies, to generate functional motor output which also combines linearly. It was also shown that in production of isometric force at the finger tip, subjects scales the level of a specific muscle activation, one that generates maximum force in given direction, pattern to scale the level of the output force in specific direction (Valero-Cuevas, 2000). Viability of this linear control scheme using modular inputs, although with simple models, has been demonstrated in other simulation studies (Raasch and Zajac, 1999; Kargo et al., 2009; Berniker et al., 2009).

Our results imply that if any selected muscle activation pattern is functionally stable, the level of the output such as limb endpoint force can be controlled by modifying the level of activation of the muscle activation pattern, simplifying the control problem In postural control, the goal of maintaining balance is to keep the CoM within the base of support. Both in cats and humans, this is done by generating proper force against the ground at each of the limb endpoint which results in net force and moment about the CoM and controls the kinematics of CoM (Ting, 2007; Lockhart and Ting, 2007). The control of muscle synergies, rather than individual muscles, in this particular aspect is supported by the fact that the biomechanical functions of individual muscles depend largely on the conditions of joints that the muscles do not cross (van Antwerp et al., 2007), suggesting more stable function could be obtained by encoding groups of muscles rather than individual muscles. Therefore, if functional stability guarantees that production of endpoint forces can be consistent over certain range, the nervous system can control the forces generated at the ground by linearly scaling and combining the muscle activation patterns. Although not readily extensible to more dynamic behaviors

with large range of joint movement such as walking, we suggest that the nervous system uses functionally stable muscle activation patterns for postural muscle synergies.

CHAPTER 5

CONCLUSION

5.1 Concluding remark

In this study, we have established a metric that can be used as the criteria for assessing functional stability of a biomechanical system under particular muscle activation. The result showed that the specified criteria for functional stability are effective in terms of predicting the behavior described by the joint configuration and endpoint force production in a consistent manner. As been demonstrated, we have further shown that muscle activation pattern based on minimum-effort for five active force vectors that is used in cat postural balance can be functionally stable and unstable and also that eigenvalue and eigenvector of the linearized system could predict the time scale and the mode of how system is driven unstable when perturbed from original equilibrium. Based on our findings from this study, we conclude that functional stability is useful in assessing stability of the biomechanical system in the context of the physiological behavior of postural control. Also, when selecting a specific muscle activation pattern for required movement, either the nervous system or an engineer needs to take into account of functional stability which can be predicted from our approach used in this study.

5.2 Future Work

More work need to be done to show that effectiveness of functional stability holds in more realistic, challenging condition. For example, gravity which was excluded from this study may or may not make the system more unstable under constant acceleration at the body segments. Also, more degrees of freedom can be allowed to the system. For example, the pelvis can be allowed to move and represented as a mass connected to a

fixed point by spring. Moreover, compared to the assumption of this study where synergy force vectors are regarded as static force, temporal modulation of activation level using multiple muscle activation patterns in combination can be done. Finally, dynamic perturbation can be applied to the hinlimb model where toe position could be displaced as in the real cat experiments or external force/acceleration can be applied to any body segments. This way, our analysis can be extended in general applicability for evaluating functional stability of a given muscle activation pattern in other models and motor tasks.

Lastly, incorporating the knowledge of intrinsic muscle properties and dominant unstable mode with linearized system, we can establish a search with a cost function that encapsulates both stability and effort. Based on our results, we further suggest several plausible approaches that seek to find muscle activation pattern that is functionally more stable and issues that may open more research questions.

- Because some postural muscle synergies were already functionally stable we can start from the minimum-effort solution and modify the activation pattern within the null-space for static torque requirement. A specific joint can be stiffened, based on the relative magnitude of each component in the unstable eigenvectors which represent the mode of how states behave unstable.
- A muscle pattern can be chosen from the task-relevant space by preferentially recruiting the muscles that are insensitive in terms of the fiber length changes and consequently the production of its output force, while ensuring stiffness provided by co-activation in the null-space. However, change in fiber length is also dependent on the type and level of perturbation. Given that muscles show directional tuning in their response to perturbations, this may open more questions related to the spatial organization of muscle activation patterns.
- Finally, one can explicitly formulate a cost function that takes into account both effort and stability. Because we can predict the behavior based on eigenvalues and eigenvectors, we can drive the search to find muscle activation pattern that closely

resembles or avoids specified eigenvalues and eigenvectors. Practically, for a given posture, state matrix can be obtained most efficiently for the muscle model used in this study using NEUROMECHANIC.

REFERENCES

Aithaddou R, Jinha A, Herzog W, and Binding P. Analysis of the force-sharing problem using an optimization model. *Mathematical Biosciences* 191: 111-122, 2004.

Alexander RM. Optimization and gaits in the locomotion of vertebrates. *Physiological Reviews* 69: 1199-1227, 1989.

Alexander RM. Models and the scaling of energy costs for locomotion. *J. Exp. Biol.* 208: 1645-1652, 2005.

Berniker M, Jarc A, Bizzi E, and Tresch MC. Simplified and effective motor control based on muscle synergies to exploit musculoskeletal dynamics. *Proc Natl Acad Sci U S A* 106: 7601-7606, 2009.

Bernstein N. *The Coordination and Regulation of Movements*. New York: Pergamon Press, 1967.

Bunderson NE, Burkholder TJ, and Ting LH. Reduction of neuromuscular redundancy for postural force generation using an intrinsic stability criterion. *J Biomech* 2008.

Bunderson NE, McKay JL, Ting LH, and Burkholder TJ. Directional constraint of endpoint force emerges from hindlimb anatomy. *J Exp Biol* 213: 2131-2141, 2010.

Burkholder TJ, and Nichols TR. The mechanical action of proprioceptive length feedback in a model of cat hindlimb. *Motor Control* 4: 201-220, 2000.

Burkholder TJ, and Nichols TR. Three-dimensional model of the feline hindlimb. *Journal of Morphology* 261: 118-129, 2004.

Carlsöö S. *How Man Moves*. London: Heinemann, 1972.

Chvatal SA, Torres-Oviedo G, Safavynia SA, Ting LH. Common muscle synergies for control of center of mass and force in nonstepping and stepping postural behaviors. *J Neurophysiol* 106: in press, 2011.

Crowninshield RD, and Brand RA. A physiologically based criterion of muscle force prediction in locomotion. *J Biomech* 14: 793-801, 1981.

d'Avella A. Control of Fast-Reaching Movements by Muscle Synergy Combinations. *J Neurosci* 26: 7791-7810, 2006.

d'Avella A, and Bizzi E. Shared and specific muscle synergies in natural motor behaviors. *Proc Natl Acad Sci U S A* 102: 3076-3081, 2005.

d'Avella A, Saltiel P, and Bizzi E. Combinations of muscle synergies in the construction of a natural motor behavior. *Nat Neurosci* 6: 300-308, 2003.

Delp SL, Anderson FC, Arnold AS, Loan P, Habib A, et al. OpenSim: Open38 source software to create and analyze dynamic simulations of movement. IEEE, 2007.

Drew T, Kalaska J, and Krouchev N. Muscle synergies during locomotion in the cat: a model for motor cortex control. *J Physiol* 586: 1239-1245, 2008.

Elble RJ, Moody C, Leffler K and Sinha R. The initiation of normal walking. *Mov Disord* 9:139–146, 1994.

Erdemir A, McLean S, Herzog W, and van den Bogert AJ. Model-based estimation of muscle forces exerted during movements. *Clinical Biomechanics* 22: 131-154, 2007.

Franklin DW, Burdet E, Tee KP, Osu R, Chew CM, Milner TE, and Kawato M. CNS learns stable, accurate, and efficient movements using a simple algorithm. *J Neurosci* 28: 11165-11173, 2008.

Fung J, and Macpherson JM. Determinants of Postural Orientation in Quadrupedal Stance. *J Neurosci* 15: 1121-1131, 1995.

Ganesh G, Haruno M, Kawato M, and Burdet E. Motor memory and local minimization of error and effort, not global optimization, determine motor behavior. *J Neurophysiol* 104: 382-390, 2010.

Gordon AM, Huxley AF, and Julian FJ. The variation in isometric tension with sarcomere length in vertebrate muscle fibres. *J Physiol* 184: 170-192, 1966.

Hart CB, and Giszter SF. Modular Premotor Drives and Unit Bursts as Primitives for Frog Motor Behaviors. *J Neurosci* 24: 5269-5282, 2004.

Harwood MR, Mezey LE, and Harris CM. The spectral main sequence of human saccades. *J. Neurosci* 19:9098–9106, 1999.

Hasan Z. The human motor control system's response to mechanical perturbation: should it, can it, and does it ensure stability? *J Mot Behav* 37: 484-493, 2005.

Henry SM, Fung J, and Horak FB. EMG responses to maintain stance during multidirectional surface translations. *J Neurophysiol* 80: 1939-1950, 1998.

Hoyt DF, and Taylor CR. Gait and the energetics of locomotion in horses. *Nature* 292: 239-240, 1981.

Hunter LC, Hendrix EC, and Dean JC. The cost of walking downhill: Is the preferred gait energetically optimal? *J Biomech* 43: 1910-1915, 2010.

Ivanenko YP, Cappellini G, Dominici N, Poppele RE, and Lacquaniti F. Coordination of locomotion with voluntary movements in humans. *J Neurosci* 25: 7238-7253, 2005.

Jacobs R, and Macpherson JM. Two functional muscle groupings during postural equilibrium tasks in standing cats. *J Neurophysiol* 76: 2402-2411, 1996.

Jinha A, Ait-Haddou R, and Herzog W. Predictions of co-contraction depend critically on degrees-of-freedom in the musculoskeletal model. *J Biomech* 39: 1145-1152, 2006.

Kargo WJ, Ramakrishnan A, Hart CB, Rome LC, and Giszter SF. A simple experimentally based model using proprioceptive regulation of motor primitives captures adjusted trajectory formation in spinal frogs. *J Neurophysiol* 103: 573-590, 2010.

Kistemaker DA, Wong JD, and Gribble PL. The Central Nervous System Does Not Minimize Energy Cost in Arm Movements. *J Neurophysiol* 104: 2985-2994, 2010.

Kuo AD. A least-squares estimation approach to improving the precision of inverse dynamics computations. *J Biomech Eng* 120: 148–159, 1998.

Li G, Kaufman KR, Chao EY, Rubash HE. Prediction of antagonistic muscle forces using inverse dynamic optimization during flexion/extension of the knee. *J Biomech Eng* 121: 316–322, 1999.

Lockhart DB, and Ting LH. Optimal sensorimotor transformations for balance. *Nat Neurosci* 10: 1329-1336, 2007.

Macpherson JM. Strategies that simplify the control of quadrupedal stance. II. Electromyographic activity. *J Neurophysiol* 60: 218-231, 1988.

Mann RA, Hagey JL, White V and Liddell D. The initiation of gait. *J Bone Joint Surg* 61-a: 232–239, 1979.

McKay JL, Burkholder TJ, and Ting LH. Biomechanical capabilities influence postural control strategies in the cat hindlimb. *J Biomech* 40: 2254-2260, 2007.

McKay JL, and Ting LH. Functional muscle synergies constrain force production during postural tasks. *J Biomech* 41: 299-306, 2008.

Nelson WL. Physical principles for economies of skilled movements. *Biol. Cybern.* 46: 135–147, 1983.

Raasch CC, and Zajac FE. Locomotor strategy for pedaling: Muscle groups and biomechanical functions. *J Neurophysiol* 82: 515-525, 1999.

Raasch CC, Zajac FE, Ma B, and Levine WS. Muscle coordination of maximum-speed pedaling. *J Biomech* 30: 595-602, 1997.

Thelen DG, and Anderson FC. Using computed muscle control to generate forward dynamic simulations of human walking from experimental data. *J Biomech* 39: 1107-1115, 2006.

Thelen DG, Anderson FC, and Delp SL. Generating dynamic simulations of movement using computed muscle control. *J Biomech* 36: 321-328, 2003.

Ting LH, and Macpherson JM. A Limited Set of Muscle Synergies for Force Control During a Postural Task. *J Neurophysiol* 93: 609-613, 2004a.

Ting LH, and Macpherson JM. A limited set of muscle synergies for force control during a postural task. *J Neurophysiol* 93: 609-613, 2005.

Ting LH, and Macpherson JM. Ratio of shear to load ground-reaction force may underlie the directional tuning of the automatic postural response to rotation and translation. *J Neurophysiol* 92: 808-823, 2004b.

Ting LH, and McKay JL. Neuromechanics of muscle synergies for posture and movement. *Curr Opin Neurobiol* 17: 622-628, 2007.

Todorov E. Optimality principles in sensorimotor control. *Nat Neurosci* 7: 907-915, 2004.

Torres-Oviedo G, Macpherson JM, and Ting LH. Muscle synergy organization is robust across a variety of postural perturbations. *J Neurophysiol* 96: 1530-1546, 2006.

Torres-Oviedo G, and Ting LH. Muscle synergies characterizing human postural responses. *J Neurophysiol* 98: 2144-2156, 2007.

Torres-Oviedo G, and Ting LH. Subject-specific muscle synergies in human balance control are consistent across different biomechanical contexts. *J Neurophysiol* 103: 3084-3098, 2010.

Tresch MC, Cheung VC, and d'Avella A. Matrix factorization algorithms for the identification of muscle synergies: evaluation on simulated and experimental data sets. *J Neurophysiol* 95: 2199-2212, 2006.

Tresch MC, Saltiel P, and Bizzi E. The construction of movement by the spinal cord. *Nat Neurosci* 2: 162-167, 1999.

Valero-Cuevas FJ. A mathematical approach to the mechanical capabilities of limbs and fingers. *Adv Exp Med Biol* 629: 619-633, 2009.

Valero-Cuevas FJ. Predictive modulation of muscle coordination pattern magnitude scales fingertip force magnitude over the voluntary range. *J Neurophysiol* 83: 1469-1479, 2000.

van Antwerp KW, Burkholder TJ, and Ting LH. Inter-joint coupling effects on muscle contributions to endpoint force and acceleration in a musculoskeletal model of the cat hindlimb. *J Biomech* 40: 3570-3579, 2007.

Vaughan CL, Andrews JG and Hay JG. Selection of body segment parameters by optimization methods. *J Biomech Eng* 104: 38–44, 1982.

Winter DA. *The Biomechanics and Motor Control of Human Gait*. Waterloo, Ontario, Canada: University of Waterloo Press, 1987.

Winter DA, and Yack HJ. EMG profiles during normal human walking: stride-to-stride and inter-subject variability. *Electroencephalogr Clin Neurophysiol* 67: 402-411, 1987.

Zajac FE. Muscle and tendon: properties, models, scaling, and application to biomechanics and motor control. *Crit Rev Biomed Eng* 17: 359-411, 1989.